I.U.S.S.
Istituto Universitario
di Studi Superiori

Università degli
Studi di Pavia

EUROPEAN SCHOOL OF ADVANCED STUDIES IN REDUCTION OF SEISMIC RISK

ROSE SCHOOL

3D PUSHOVER OF IRREGULAR REINFORCED CONCRETE BUILDINGS

A Dissertation Submitted in Partial Fulfillment of the Requirements for the Master Degree in

EARTHQUAKE ENGINEERING

By

MANUEL ALFREDO LOPEZ MENJIVAR

Supervisor: Dr RUI PINHO

September, 2003

The dissertation entitled “3D pushover of irregular reinforced concrete buildings”, by Manuel Alfredo López Menjivar, has been approved in partial fulfilment of the requirements for the Master Degree in Earthquake Engineering.

Rui Pinho

Alberto Pavese

ABSTRACT

Seismic response of irregular plan buildings can be assessed by using time history analysis; however, this process is, in general, lengthy and has to be repeated many times to have a wide set of results that could represent the performance of the system facing any seismic excitation. Obviously, such procedure may take up considerable time before significant and useful data is obtained in the analysis of an irregular system; therefore, some other procedures, less time consuming and equally reliable, have been developed, one of them is the pushover analysis. Pushover is a tool that is widely used to predict the strength and response of 2D frames.

Currently, in this research, the methodology is extended to assess the performance of 3D irregular RC structures. Important issues regarding diaphragm effects, direction of load application, loading profiles and arrangement of the incremental dynamic analysis results have been studied; in addition, the capability of adaptive pushover has been tried. Two RC irregular buildings and six earthquake ground motions were employed throughout the research. From the processing of the above information preliminary conclusions are drawn and future lines of research are proposed.

ACKNOWLEDGEMENTS

To Julian Bommer, who always has been an example to follow as researcher and professor, because he introduced me to the ROSE's world and pushed me to be part of it.

To Mario Nieto for his immense tolerance and patience for bearing with my decision to study abroad once more.

To my family because their support to my cause in all senses.

To Dr. Rui Pinho, for being an outstanding professional guide and an amazing hard-working person, who is ready to help facing any situation and to Dr. Alberto Pavese for his invaluable aid.

To Prof Calvi for giving me the opportunity to be part of ROSE School, to ROSE faculty for their instruction, to the personnel of Dipartimento di Meccanica Strutturale dell Universita' degli Studi di Pavia for their helpfulness, and the last but not the least to Sandra Castelli who personally takes care of each one of the ROSE students.

To ROSE friends for their companionship which makes the load less heavy.

AGRADECIMIENTOS

A Julian Bommer, quien siempre ha sido un ejemplo a seguir tanto como investigador y profesor, debido a que fue él quien me habló del mundo de ROSE y me alento a ser parte de el.

A Mario Nieto por su inmensa tolerancia y paciencia para soportar mi decisión de continuar estudiando.

A mi familia por su apoyo, en todos los sentidos, a mi causa.

Al Dr. Rui Pinho, por ser un profesional brillante y un increible trabajador, quien esta siempre dispuesto a ayudar en cualquier situación; asimismo, al Dr. Alberto Pavese por su invaluable ayuda.

Al Prof. Calvi por darme la oportunidad de ser parte de ROSE School, al personal del Dipartimento di Meccanica Strutturale dell Universita' degli Studi di Pavia por su colaboración, y en especial a Sandra Castelli quien hace que todo el engranaje operativo de ROSE funcione.

A mis amigos en ROSE quienes con su amistad hacen la carga menos pesada.

3D ADAPTIVE PUSHOVER OF REINFORCED CONCRETE BUILDINGS

INDEX

page

LIST OF TABLES

LIST OF FIGURES

1. INTRODUCTION

There have been many attempts to predict the dynamic behavior of 3D irregular buildings by simpler methods than using time history analysis. An important shortcoming with many of the methodologies presently used is that they have been developed for single storey structures and their results have been extended to multistory regular buildings. However, it is doubtful this analogy could be applied to irregular buildings mainly because studies using single storey models do not account for complex dynamic response and high order effects. One of the most utilized approaches in the 2D buildings is the conventional pushover which has been extended to the analysis of 3D structures.

Although the 3D pushover analysis might appear to be an appealing methodology and easy task to perform, it may involve some issues that need answers before its results can be considered reliable. Issues such as: How the contribution of the slab should be modeled? Rigid?, Flexible? or Partially flexible?; Which type of pushover should be used? Conventional? or Adaptive?; If conventional is decided to be used, which load profile to use? Triangular? or Uniform?; If adaptive is selected, then which scheme to employ? Force-based? or Displacement-based?. However, at some point the concern of assessing pushover accuracy arises, but that topic is readily solved by matching up to this static method with the incremental dynamic analysis. But, this comparison produces new issues to be defined such as: How to match the pushover results with the incremental dynamic analysis results? By using capacity curve (displacement vs. base shear)?, by using drift profiles?, by using shear profiles? or all of them?; if capacity curves are used, then which displacement-base shear arrangement (of the dynamic results) would be chosen? Maximum displacement vs. maximum base shear, independently of the time of occurrence?, Maximum displacement vs. corresponding base shear, in the same occurrence time? or Maximum base shear vs. corresponding displacement, in the same time of occurrence? and Which locations to study? Center of mass?, rigid edge?, flexible edge? or all of

them?; furthermore, if drift profiles are employed, at which instant will those be computed?; and, at which locations?. Thus, as it has been seen, the pushover analysis is not a simple theme to deal with.

To tackle the above issues an introductory study was performed which results are presented in the current document. The methodology adopted was the following: Two irregular reinforced concrete building were analyzed; modeling was carried out by using fiber analysis approach; three types of analyses were executed, conventional and adaptive pushovers and incremental dynamic analysis. Once the data is obtained, comparisons among the three analyses were performed and preliminary conclusions were drawn. Since the present work is an introductory study, further lines of research are proposed.

1.1 DISSERTATION OUTLINE

In the second chapter of this dissertation a literature review is carried out. Different pushover procedures, to study the behavior of irregular plan buildings, are presented which range from early attempts by using two-dimension conventional pushover to the current efforts by employing three dimension adaptive pushover.

The third chapter is concerned with the modeling approach used in the discretization of the selected structures as well as the performed analyses applied to the models.

In chapter fourth some results are presented such as dynamic characteristics of the models, diaphragm effects, incremental dynamic analysis, appropriate direction of static load application, best loading profile for conventional and adaptive pushover and the comparison among the incremental dynamic analysis, conventional pushover analysis and adaptive pushover analysis.

Chapter fifth compiles the conclusions obtained from the preceding chapters and draws some ideas to improve the present research. This dissertation finishes listing the references employed during the study, at chapter sixth.

2. THEORETICAL BACKGROUND

2.1 INTRODUCTION

Torsional effects on buildings produced by irregularity in mass, stiffness or strength distribution has been tackle using different approaches. The most used and simplest one, the methodology proposed by buildings codes where by moving the application point of the applied static load, on the plan of each floor, the torsion is supposedly taken into account. Eccentricities are employed to quantify that movement and the concept was introduced to estimate the seismically induced displacement at the two critical edges of a building, namely the flexible edge and the stiff edge [Lam *et al.*, 1997]. This methodology has been developed based on single story models and its results can be extended to regular multi story buildings; nonetheless, it is doubtful that analogy could be extended to irregular systems, mainly because the static force method does not account for complex dynamic response and high order effects [Lam *et al.*, 1997]. Since the expressions presented on building codes may not represent the torsional effects, there have been numerous attempts to produce methodologies that cover the flaws from the above procedure, a number of which still study one floor systems and attempt to extrapolate the results to irregular multistory systems; some others utilize displacement-based concepts but they are rather oriented to design than to analyze; and some others make use of pushover analysis to accomplish the task.

2.2 LITERATURE REVIEW

Following the pushover approach, there have been many attempts to develop a simple method, yet capable, to predict seismic response of irregular buildings. One of the earliest efforts was done by Moghadam and Tso [1996] where the application of two static pushovers combined with a dynamic analysis of a single degree of freedom system was used to estimate the seismic deformation and damages of elements located at the perimeter of the building. The methodology starts with a pushover analysis of the three dimensional system from which base shear- roof center of mass displacement

relationship is obtained; such correlation is approximated by a bilinear hysteretic curve, to account for unloading. Subsequently, a SDOF system is developed by means of the deflection profile, of the 3D model, when the top center of mass displacement equals to 1% of the total height; then, a non linear dynamic analysis of the SDOF system is performed to obtain the maximum center of mass displacement of the roof of the structure, Y_{max}. Subsequently, another 3-D pushover analysis is then carried out to determine the state of stress and deformation of the flexible edge of the building when the top center of mass displacement equals to the Y_{max}. It is assumed that the deformations and damages on elements close or at the flexible edge of the model, obtained by the above procedure, represent both effects on the actual structure when the building is subjected to a particular earthquake.

The approach previously highlighted seems to produce comparable results with those from the dynamic analysis when maximum roof displacement at center of mass is evaluated; however, poor predictions of the top displacement of the flexible edge and maximum interstory drift at that location are obtained, especially when near field records were used. Likewise, maximum ductility demands in beams and columns at the flexible edge frame presented poor correlation in cases where near field motions were used. No results from the stiff side of the building are presented. The main supposition behind the methodology is that the building would behave essentially in a single mode during an earthquake; obviously, that assumption is an important shortcoming in the process because more than one mode may have contribution in the response of irregular structures, particularly when the process is in high levels of inelastic behavior. A point to be highlighted is the time history analysis, to which the proposed methodology is compared, considers excitation from just one direction; this fact, as it has been pointed out in other researches [De La Colina, 1999], can produce unreliable responses, displacements especially.

Subsequently, Moghadam and Tso [2000] proposed a modified approach to account for torsional effects on irregular buildings. In this new methodology, the target displacement is obtained by performing an elastic spectrum analysis of the building; since the top displacements of different resistant elements are different, many target displacements need to be computed. The lateral load distributions used in the pushover are taken from the spectrum analysis, as well, to take into account the high order effects. With the target deformation and the load distribution fixed up, 2D pushover analyses of the selected elements are carried out. The elements are pushed until the target displacements, per each one, are achieved. Three different building configurations are used, to test the scheme, uniform moment resisting frame, set-back moment resisting frame and uniform wall-frame buildings. An ensemble of 10 artificial ground motion records, with response spectrum shapes similar to the Newmark-Hall design spectrum, are developed to run the time history analyses. The authors claim that this methodology works well in the uniformed moment resistant frame system, especially in the local response parameters (results not shown in the article); however, the pushover results for the

other two systems are not well correlated with the time history results. Again, the proposed methodology, although, considers a different load distribution from a triangular one, it keeps a fixed load profile during the pushover process neglecting changes in the mode shapes due to inelasticity; in addition, the bidirectional excitation in the time history analysis is still not considered.

Kilar and Fajfar [1996] suggested another approach to tackle the pushover analysis on irregular structures. The starting point of the process is to create a pseudo three dimensional mathematical model which consists of assemblages of two-dimensional macroelements, or substructures, which account for walls, frames, couple walls and walls on columns, figure 2.1.

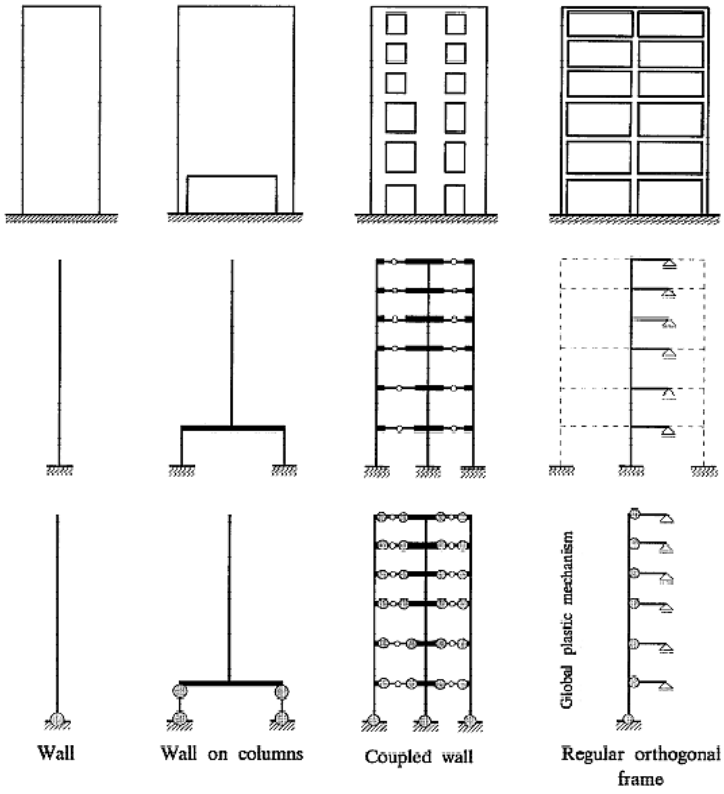

Figure 2.1. "Standard" macroelements, mathematical models for elastic analysis and assumed plastic mechanism. [Kilar and Fajfar, 1996].

These macroelements may be oriented arbitrarily in plane and are assumed to resist loads only on their plane. Then, force-displacement relationships are developed, for the four standard macrolements mentioned previously, base on the initial stiffness, strength at the assumed plastic mechanism and assumed post-yielding stiffness. Afterward, analysis is performed as a sequence of linear analyses, using event to event strategy. An event is defined as a discrete change of the structural stiffness due to the formation of a plastic hinge (or simultaneous formation of several plastic hinges) in a macroelement. The authors claim that this procedure can be used to analyze building structures of any material; however, the example presented is the comparison between a symmetric and an asymmetric

reinforced concrete buildings. The results showed were limited to compare the macroelement failure sequence in both structures and to present a plot base shear-top displacement relationship for both structures. It was concluded that larger displacement and larger ductilities are required in the asymmetric structures in order to develop the same strength as that of its symmetric counterpart. Although the proposed scheme seems simple it does not take into account high mode affecting the behavior of the building since the pushover used a fixed load profile in the shape of an inverted triangle.

Faella and Kilar [1998] using a conventional pushover, with triangular load distribution, investigated the applicability of such approach on the analysis of asymmetric plan structures. The innovation proposed was to move the load application point to fit the results from the dynamic analysis. The authors tried four possibilities, Center of Mass (CM), CM – 0.05L, CM + 0.05L and CM + 0.15L. A single building was analyzed which originally was symmetric but by changing the position of the Center of Mass became asymmetric. The results obtained were that the deflection profile both on the stiff and flexible edge could be successfully matched by shifting the point of lateral load application. In particular, it was found that, in many cases, the dynamic response profile can be enveloped by shifting the equivalent static forces at the minimum and maximum eccentricities used in the research, figure 2.2.

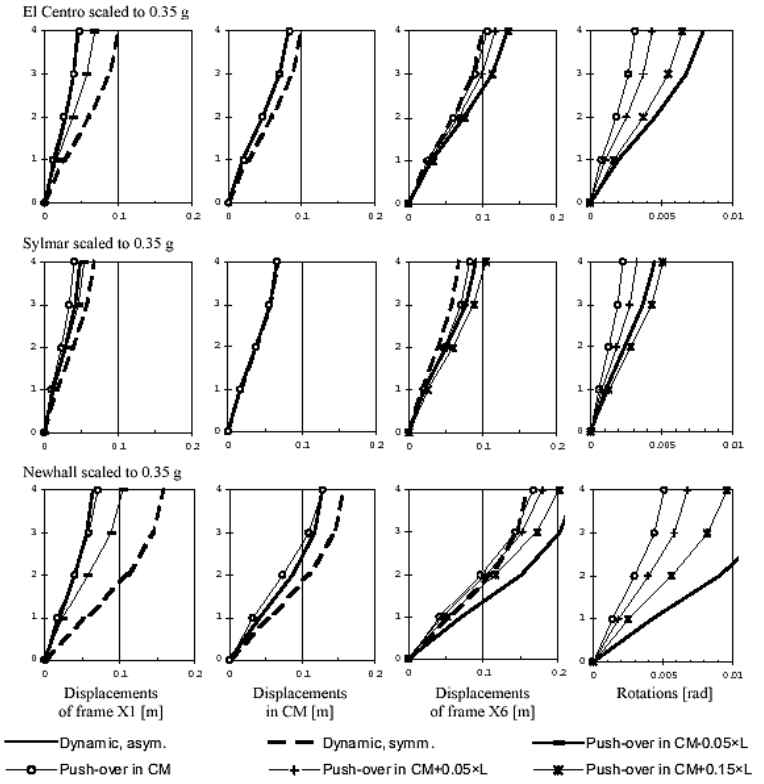

Figure 2.2. Stiff edge, CM and flexible edge deflection profiles: push-over analysis with various points of applications of lateral loads versus dynamic analysis, top displacements are measure at CM, earthquakes records scaled to 0.35g. [Faella and Kilar, 1998].

However, in all examined cases the torsional rotations obtained by dynamic analysis were much bigger than those obtained by pushover analysis even by using the largest eccentricity as the point of application; Nevertheless, since the maximum displacement at the edges of the structure does not occur at the time when the torsional rotation is maxima, the researches concluded that the failure of the pushvover in capturing such effect did not significantly affect the response of the studied building. Another finding was that the pushover results matched, or not, the dynamic results based on the intensity of the applied ground motion. An interesting conclusion can be drawn from this research, although a fixed load distribution is used deflection profiles can be matched by changing the application point, suggesting the use of adaptive patterns [Antoniou & Pinho, 2003a].

By 2002, Kilar and Fajfar explored the possibility of extending the N2 method, originally formulated for planar analysis, to the analysis of irregular structures. In addition, comparisons among N2 method, the MT method (proposed by Moghadam and Tso) and nonlinear dynamic analyses were carried out. The modified N2 procedure consists in two independent pushover analyses of the studied 3D structural model with lateral loading in both horizontal directions, respectively. Loading is applied at the mass centers. Displacement demand in the mass center at the top is determined for each direction separately, similarly to the approach used in planar N2 analysis. Finally, the deformation quantities (displacements, story drift, rotations, ductilities, etc.) are determined by a SRSS combination of effects obtained from the pushover analyses in the two directions. The authors claimed that the extension of the N2 approach seems to be able to predict the response of a torsionally stiff multi-storey asymmetric building with a reasonable accuracy, within the limits set by the dispersion of results of dynamic analyses performed with different ground motions; however, the extreme cases of plan-wise highly irregular structures were generally not appropriate for these simplified methods.

The results presented in the paper demonstrated that, for highly asymmetric structures, the N2 method overestimates the displacements at CM as well as at the flexible side, and underestimates the displacements at the stiff edge. For instance, the building presented in figure 3.9 has been studied without wall C (original structure) and with the inclusion of wall C (structure with new wall); some results are presented in table 2.1. From there it can be stated the displacements of the flexible edge (frame Y1) and the center of mass are overestimated and the displacement of the stiff edge is underestimated in both building variants while the MT method provides similar results to the N2 method, for this particular case, but the displacement of the stiff edge is overestimated, as well.

As noted earlier the MT was tested equally by Kilar and Fajfar [2002]. It was found the method provided reasonably accurate results for structures, regular in elevation and composed of similar load-bearing elements; nevertheless, the MT approach, which is based on elastic dynamic analysis, did not

adequately represent the inelastic structural behavior in the case of structures where significant strength redistribution may be expected during nonlinear excursions. It has to be pointed out that results from both N2 and MT methodologies are based on the elastic stiffness of the structure; however, the MT method does not make available a clear information in how to obtain the effective elastic stiffness, opposed to the N2 method in which the elastic stiffness is determined based on a bilinear approximation of the pushover curve.

Table 2.1. Maximum top displacements obtained by nonlinear dynamic analysis (average values) and simplified methods (cm). Values in parentheses represent percentages of corresponding values obtained by dynamic analysis. Stiff side is represented by frame Y1 and wall B; flexible side is represented by frame Y5. [Kilar and Fajfar, 2002].

ORIGINAL STRUCTURE

	Y1	WALL B	CM (Y)	Y5	CM (X)	X4	Rotation
DYNA (100%)	1.3	3.2	10.9	22.4	19.9	22.0	0.0094
N2 (const.)	0.7 (51%)	3.8 (118%)	14.6 (134%)	28.5 (127%)	22.2 (112%)	23.2 (105%)	0.0112 (119%)
N2 (1. mode)	0.6 (46%)	4.3 (134%)	17.3 (159%)	33.9 (151%)	23.3 (117%)	23.8 (108%)	0.0134 (143%)
MT	2.4 (185%)	3.2 (100%)	13.9 (128%)	28.6 (128%)	24.0 (121%)	24.8 (113%)	0.0119 (127%)

STRUCTURE WITH NEW WALL

	Y1	WALL B	CM (Y)	WALL C	Y5	CM (X)	X4	Rotation
DYNA (100%)	1.4	2.4	9.2	16.3	18.5	19.3	21.8	0.0076
N2 (const.)	0.9 (64%)	3.3 (137%)	11.8 (128%)	20.1 (123%)	22.7 (122%)	22.2 (115%)	22.9 (105%)	0.0088 (116%)
MT	6.8 (489%)	7.2 (300%)	13.4 (197%)	21.1 (129%)	23.7 (128%)	24.0 (124%)	24.3 (111%)	0.0091 (120%)

Penelis and Kappos [2002] aimed to develop a method that allow the modeling of the torsional response of building using 3D pushover analysis which results does not deviate from those of time history analysis. The methodology proposes to build the mean elastic spectrum from a set of times histories previously scaled according to the PGA or spectrum intensity. With the mean elastic spectrum a dynamic response spectrum analysis is performed on the selected building, from which the translation and torque at the center of mass are calculated. Based on those two values and on an elastic static analysis of the building the lateral force and the torque are obtained. Next, the reduction factors to convert the MDOF system to an equivalent SDOF system are calculated. Afterward, a 3D pushover analysis of the building, using the lateral force and torque previously calculated, is performed to obtain the force-deformation curve which is reduced by the factors already found at the last step to obtain the capacity curve of the equivalent SDOF system.

Both the target displacement and torsional rotation, for the SDOF system, are calculated based on the mean inelastic acceleration-displacement response spectra, obtained for several ductility factors, and on the reduced force-deformation curve; both plot are superimposed and the desired target displacement is attained. Using the reduction factors the target and torsional rotation for the MDOF system is calculated. As examples two single-storey buildings are analyzed. Reasonable correlation

between results from the time history analysis and the proposed approach can be observed in the results presented at the paper, especially for the pre-yielding stage; however, as it was pointed out before, results based on single-story models, which could well represent the behavior of regular multistory buildings, are doubtful that they could be extended to irregular systems; because, uniform multistory buildings may have the center of mass and center of stiffness vertically aligned, but in the case of irregular structures that may not be the case. This trend could worsen when the different elements in the irregular building begin to enter in the inelastic range; and the center of stiffness at each floor will be located in different positions on the plan of the structure. There is no practical application example of the methodology to a multistory building.

Antoniou and Pinho [2003a & 2003b] have developed an adaptive pushover methodology where the current stiffness state and modal properties of the structure at various levels of inelasticity are considered in order to update the lateral load distribution, either forces or displacements, in height. Such approach has been tested in two dimensional systems with success; therefore, an extension to study the response of buildings with plan irregularity is a logical step. However, before presenting analytical data and conclusions the method is explained in the next section.

2.3 THE ADAPTIVE PUSHOVER ALGORITHM

This adaptive pushover strategy, presented by Antoniou and Pinho, is fully adaptive and multi-modal. It accounts for system degradation and period elongation during the procedure by updating the force distribution at every, or predefined, step. The dynamic properties of the system are determined by means of eigenvalue analyses, which consider the instantaneous structural stiffness state, whereas a site-specific spectral shape or record can be utilized for the scaling forces, in order to account for the expected ground motion. Two variants of the method exist, Force-base Adaptive Pushover (FAP) and Displacement-base Adaptive Pushover, depending whether forces or displacements are applied.
The basic steps of the methodology are described below:

- At each step, prior to the application of any additional load, eigenvalue analysis considering the stiffness state at the end of the previous load step is performed and periods and eigenvectors are calculated. For this purpose the Lanczos method is used.
- From the modal shapes and the participation factors of the eigensolution, the patterns of the story forces (for FAP) or displacements (for DAP) are determined separately for each mode. If a particular spectral shape is considered the corresponding value for each mode of vibration is also considered in the computation of the force pattern.
- The lateral load profiles of the modes are combined by using either the Square Root of the Sum of Squares (SRSS) or the complete Quadratic Combination (CQC) method. Since only the relative values of storey force are of interest (the absolute values are determined by the

load factor λ and the nominal loads) the horizontal loads are normalized with respect to the total values, in the case of FAP, or the maximum value, for DAP.

If the eigen-solver, for any reason, fails to converge or output real eigensolutions, the two previous steps are omitted and the load pattern of the preceding increment is employed. This is the case at the highly inelastic post-peak range, where negatives values appear in the diagonal of the stiffness matrix, which lead to imaginary periods and unrealistic modal shapes.

- Update (increase) the load factor λ. The loads applied at each storey are evaluated as the product of the updated load factor, the nominal load at that storey and the force/displacement pattern obtained above (normally, the nominal loads at all storeys should be equal). Alternatively, incremental scaling can also be employed, whereby only the load increment is updated and added to the load already applied to the structure throughout the previous increments.
- Apply the new calculated forces to the model and solve the system of equations to obtain the structural response at the new equilibrium state.
- Calculate the updated tangent stiffness matrix of the structure and return to the first step of the algorithm, for the next increment of the adaptive pushover analysis.

The above algorithm has been implemented effectively in SeismoStruct [2003] analytical package, software that will be used to perform the analyses needed to verify the applicability of the adaptive pushover to irregular plan buildings. In addition, there are some other options, implemented in the package, which can be used depending on the needs of the analysis. For instance, scaling modal forces with or without the consideration of spectral amplification; choosing to update the load distribution at every step for better accuracy and stability, or at predefined steps to reduce computational time; introducing a user defined spectrum or a particular record to derive the spectral coordinates; selecting the possibility to choose either force-control or response-control schemes. More information can be found in Antoniou and Pinho [2003a].

3. MODELING OF CASE STUDIES

3.1 INTRODUCTION

In order to evaluate the capacity of the adaptive pushover to assess the behavior of irregular plan systems, two asymmetric building structures have been selected. The first one is a three storey concrete structure to be tested at the European Laboratory for Structural Assessment (ELSA) at ISPRA within the auspices of the EU project Seismic Performance Assessment and Rehabilitation (SPEAR), Fardis [2002]. The second one is a four storey building with dual system studied by Kilar and Fajfar [2002].

3.2 MODELLING APPROACH

3.2.1 Mathematical tool

The finite element analysis program SeismoStruct [2003] is utilized to run all analysis. SeismoStruct is able to predict the large displacement behavior of space frames under static or dynamic loading, taking into account both geometric nonlinearities and material inelasticity. SeismoStruct accepts static loads (either forces or displacements) as well as dynamic (accelerations) actions and has the ability to perform eigenvalues, nonlinear static pushover (conventional and adaptive), nonlinear static time-history analysis, nonlinear dynamic analysis and incremental dynamic analysis.

3.2.2 Modeling of members

Structural members have been discretized by using a beam-column model based on distributed plasticity-fiber element approach. The model takes into account geometrical nonlinearity and material inelasticity. Sources of geometrical nonlinearity considered are both local (beam-column effect) and global (large displacement/rotation effects). Since a constant generalized axial strain shape function is

assumed in the adopted cubic formulation of the element, it results that its application is only fully valid to model the nonlinear response of relatively short members and hence a number of elements (usually three to four per structural member) is required to accurate model the structural frame members. Material inelasticity is explicitly represented through the employment of a fiber modeling approach which allows for the accurate estimation of structural damage distribution, the spread of material inelasticity across the section area and along the members length. In the fiber model the sectional stress-strain state or beam-column elements is obtained through the integration of the nonlinear uniaxial stress-strain response of the individual fibers in which the section has been subdivided. If a sufficient number of fibers is employed, the distribution of material nonlinearity across the section area is accurately modeled, even in the highly elastic range, see figure 3.1.

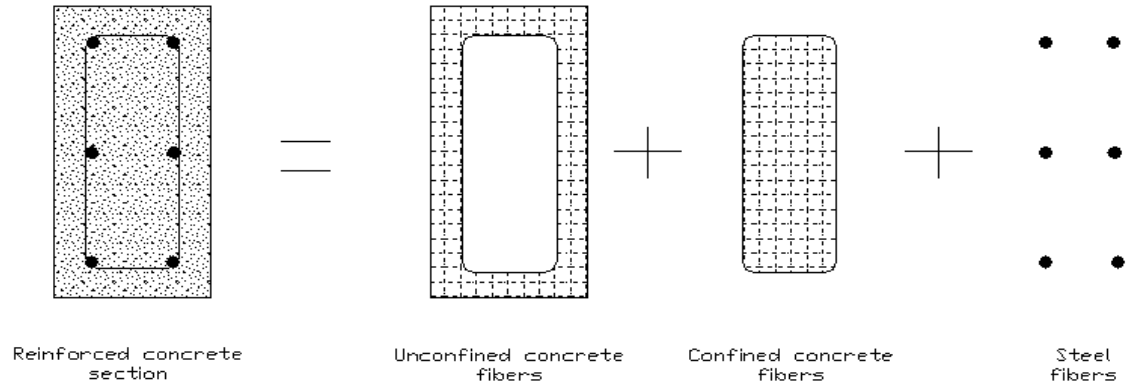

Figure 3.1. Fiber plasticity discretization in a reinforced concrete section.

The spread of inelasticity along member length then comes as a product of the inelastic cubic formulation suggested by Izzuding [2001]. Two integration Gauss points per element are used for the numerical integration of the governing equations of the cubic formulation, figure 3.2. If a sufficient number of elements is used the plastic hinge length of structural members subjected to high levels of material inelasticity can be accurately estimated.

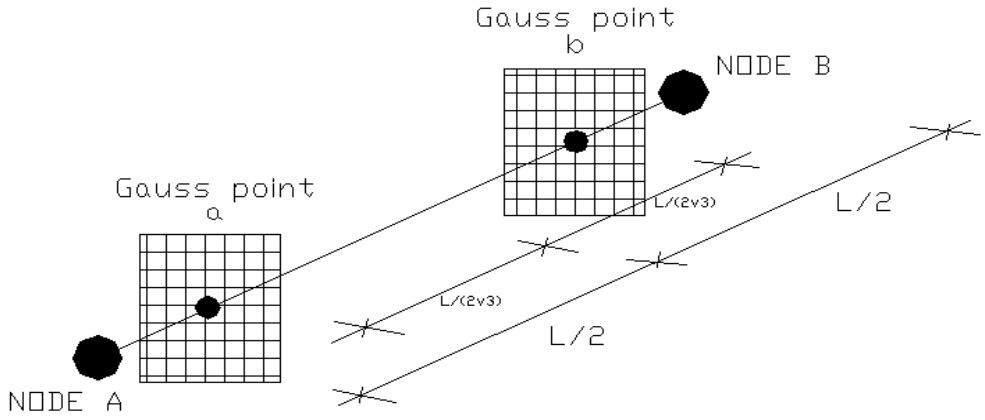

Figure 3.2. Location of Gauss points along the member length.

It is worth mentioning that at the present, shear strains across the element cross section are not modeled; in addition, warping strains and warping effects are not considered in the current formulation, either. Additionally, the elastic torsional rigidity is used in the formulation of the nonlinear frame elements; this clearly involves some degree of approximation for the case of reinforced concrete sections.

3.2.3 The SPEAR structure

The test structure is a simplification of an actual three storey building representative of older constructions in Greece, or elsewhere in the Mediterranean region, without engineered earthquake resistance. It has been designed for gravity loads alone, using the concrete design code applying in Greece between 1954 and 1995, with the construction practice and materials used in Greece in the early 70's. The structural configuration is also typical of non-earthquake-resistant construction of that period, Fardis [2002].

Plan dimensions of the structure are given in figure 3.3. The storey height is 3.0 m, from top to top of the slab. Design gravity loads on slabs are 0.5 kN/m^2 for finishing and 2 kN/m^2 for live loads. The slab has a thickness of 150 mm and is reinforced by 8 mm bars at 200 mm centers, both ways. Column longitudinal reinforcement is composed of 12 mm bars, lap spliced over 400 mm at each floor level, including the first story; spliced bars have 180° hooks. Columns transverse reinforcement are 8 mm diameters stirrups at 250 mm centers, closed with 90° hooks; stirrups do not continue into the joints. Clear cover of stirrups is 15 mm. The dimensions of most of the columns are 250 mm by 250 mm; however, there is one column with dimensions equal to 750 mm by 250 mm, see figure 3.2.

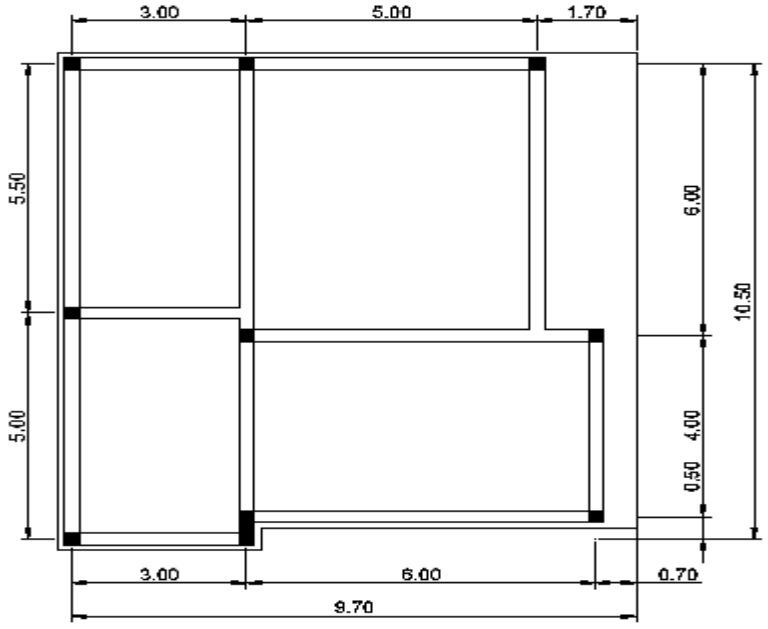

Figure 3.3. Plan view of ISPRA structure, dimensions in m.

Typical beam detailing is shown in figures 3.4 and 3.5. Beam reinforcement, at the top, is constituted by two 12 mm bars, anchored with 180° hook at far end column, without downward bent. The bottom reinforcement consists of two bars which continue straight to the supports, where they are anchored with 180° hooks at the far end of column and two bars bent up towards the support. These latter bars, over the interior columns, continue straight into the next span and, over the exterior columns, are bent down at the far end of the columns and anchorage with a 180° hook. The bottom steel could be either 12 mm bars or 20 mm bars, depending on the beam loads. Beam transverse reinforcement is 8 mm diameter stirrups separated at 200 mm centers, closed at top with 90° hooks; stirrups do not continue into the joints. A complete description of the structure can be consulted at Annex 1.

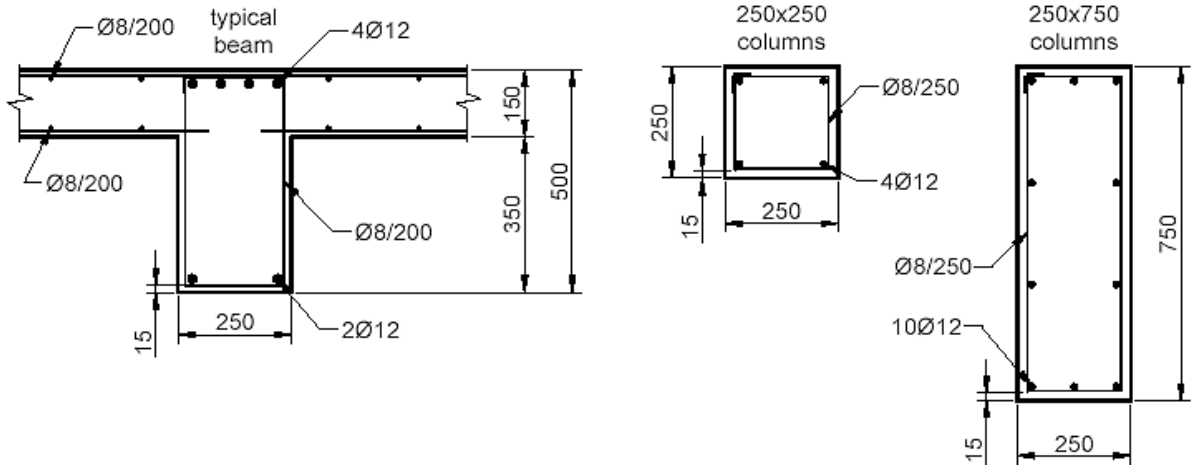

3.4. Typical beam and columns cross sections.

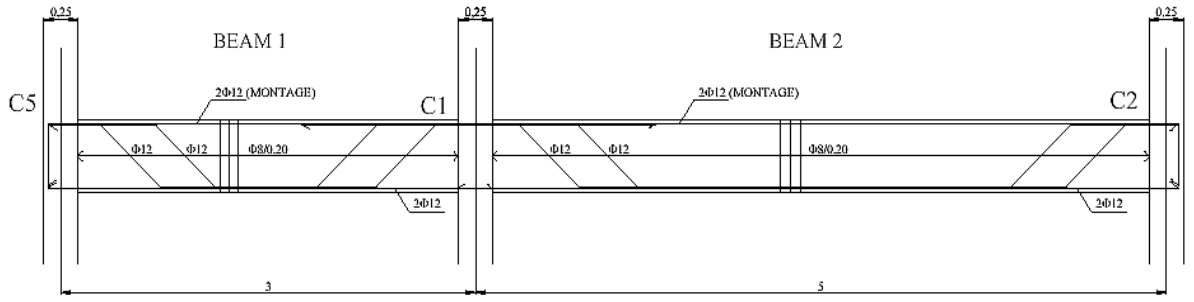

Figure 3.5. Typical beam longitudinal reinforcement.

Material properties, which were obtained from direct communication with the SPEAR project's researchers, are the following:

Table 3.1. Material mechanical characteristics of the SPEAR frame.

Unconfined concrete compression strength.	25 MPa.
Concrete strain at peak stress (Unconfined)	0.002
Steel yield strength for 12 mm bars	385 MPa
Steel maximum strength for 12 mm bars.	511 MPa
Maximum elongation at 5F baselength.	31.0%
Steel yield strength for 20 mm bars	462 MPa
Steel maximum strength for 20 mm bars.	576 MPa
Maximum elongation at 5F baselength.	29.0%

The concrete is modeled by employing a uniaxial constant confinement concrete model based on the constitutive relationship proposed by Mander *et al.*[1988] and later modified by Martinez-Rueda and Elnashai [1997] for reasons of numerical stability under larger displacement analysis. The confinement effects, provided by the lateral transverse reinforcement, are incorporated through the rules proposed by Mander et al. whereby constant confining pressure is assumed throughout the entire stress-strain range. This model is defined by four parameters: the peak compressive strength of unconfined concrete (f'_c), the tensile strength (f_t), crushing strain (ε_{co}) and the confinement factor (K). Considering that the factor K is defined as the ratio between the confined and unconfined compressive stress of the concrete and that, in the case of the SPEAR frame, the amount of transverse reinforcement of all members is very small to produce an effective concrete confinement; then, the K value has been considered 1.0 and 1.001 for unconfined and confined concrete, respectively.

Longitudinal reinforcement steel has been account by using a uniaxial steel model initially formulated by Menegotto and Pinto [1973] and later enhanced by Filippou *et al.* [1983] with the introduction of new isotropic hardening rules. It utilizes a damage modulus to represent more accurately the unloading stiffness. It is employment is advised to modeling reinforced concrete structures, particularly those subjected to complex loading histories, where significant load reversals might occur. Eight parameters have to be defined to calibrate the steel model; those are: Modulus of elasticity (E_s), yield strength (f_y), strain hardening parameter (μ), transition curve initial shape parameter (R_0), transition curve shape calibrating coefficients (a_1 & a_2) and isotropic hardening calibrating coefficients (a_3 & a_4).

Idealization of the structure is based on linear elements placed at mid-depth of the members, and connected at the nodes. Main nodes are considered where column and beam elements meet, as it is showed in figure 3.6. Each member has been further subdivided in 4 elements to effectively capture the expected inelasticity behavior, figure 3.8. For identification purposes, nodes located in the same column line share the last digits but the first digits change depending on the level where they belong. For instance, node 1 is located at the baseline, node 401, 801 and 1201 are placed at first, second and third levels, respectively, sharing the same column line of number 1, see figure 3.6.

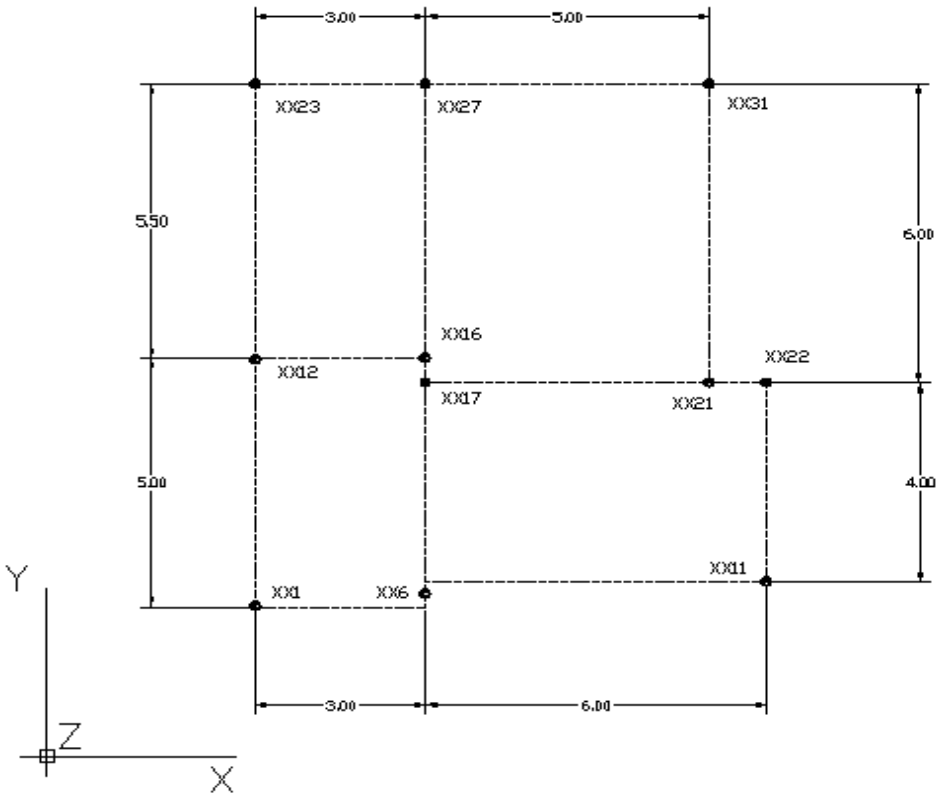

PLAN VIEW

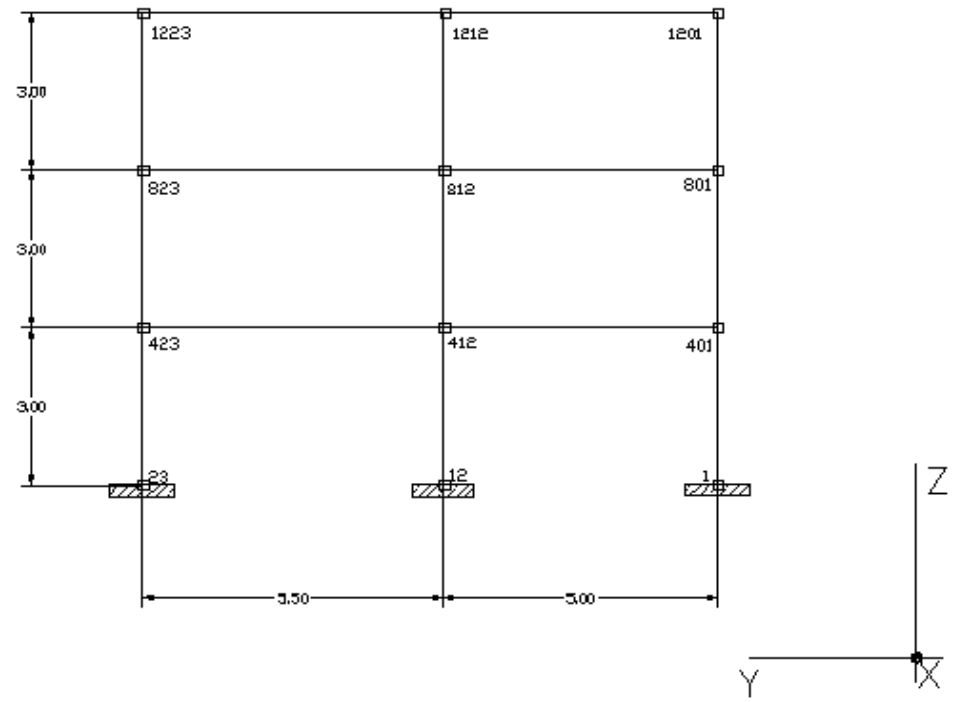

LATERAL VIEW

Figure 3.6. System of coordinates and main node numbering.

Live loads and dead load from partitions were assumed to be applied in all three stories. Self weight of reinforced concrete members and the slab was computed using a specific weight of concrete equals to 2400 kg/m^3. Gravitational loading for the seismic combination was assumed according to Eurocode [2002] as G+0.3Q, where G is the permanent load and Q is the live load. The tributary gravitational load was distributed along the frame elements. Masses were computed in similar way to that for the gravity loading and were concentrated at the nodes where columns and beams meet plus the nodes that share the code XX21. Mass value for each of the three stories is 60 Ton producing a total mass of 180 Ton.

As stated before, structural members were modeled by employing distributed plasticity fiber element approach. Centerline dimensions of elements were used to account for additional deformations not modeled directly (bar slippage, yield penetration and shear joint distortion). There was one case where rigid elements were used to connect elements; that happened at the 250X750 mm column to account for the finite dimension of the structure, see figure 3.7.

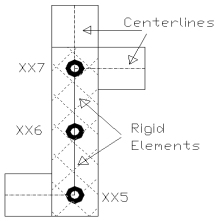

Figure 3.7. Modeling of the 250X750 mm column.

Slabs were omitted in the analytical model but their participation to the beam stiffness and strength was accounted by using the effective flange width for beams framing into columns proposed by the Eurocode 8 [2002]. The final model is presented in figure 3.8.

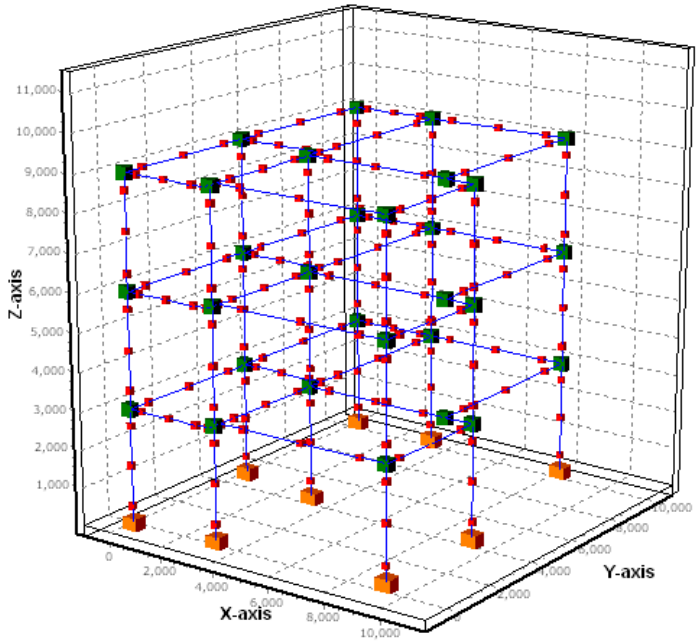

Figure 3.8. Final model of SPEAR structure.

3.2.4 RC Frame-wall building

The second structure was an existing building used in some other studies by Kilar & Fajfar [2002]. The following description has been entirely obtained from the above mentioned authors: Walls positioned on one side of the building (wall A and wall B), around the staircase, cause a large stiffness and strength eccentricity. The stiffness eccentricity amounted to approximately 40% of the larger dimension of the plan. Since the existing structure did not comply with the requirement of Eurocode 8, it was redesigned according to that standard. The dimensions of the central columns as well as the amount of the reinforcement in the majority of elements were increased. Plan and elevation views of the building are presented in figure 3.9. The cross sections of the structural members are equal in all storeys. The required different strength levels of frames due to torsion were obtained by varying the amount of reinforcement in different frames. In order to achieve uniformity of structural elements, all columns of one frame in a storey have equal reinforcement. Reinforcement does not change along the height, except for frames X2 and X3, where the reinforcement in the bottom two storeys is different from that in the upper two storeys. The frames at the flexible side (i.e. frames Y4 and Y5) have stronger reinforcement as the frames at the stiff side (i.e. frames Y1 and Y2). The frames Y2 and Y3

are identical. Identical are also frames X1 and X4, as well as frames X2 and X3. The reinforcement of walls, columns and beams is presented in Figure 3.10 and Table 3.2.

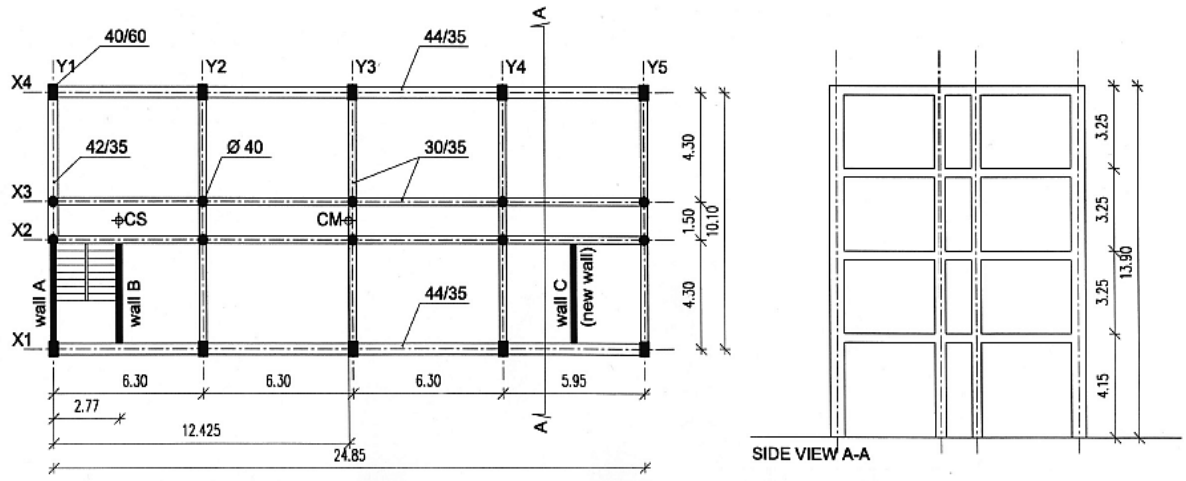

Figure 3.9. Plan and elevation views from the RC frame-wall building.

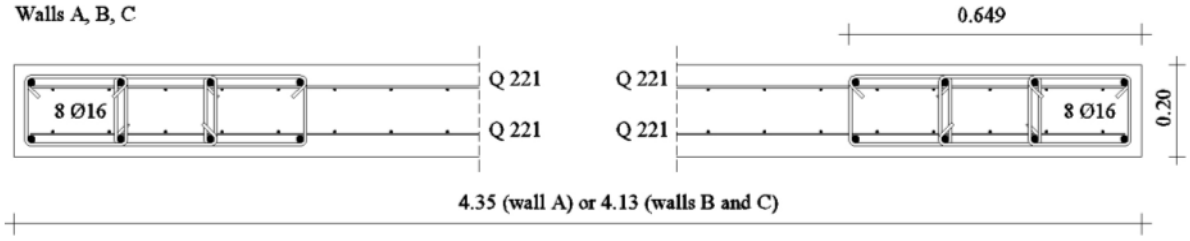

Figure 3.10. Reinforcement of walls (Q221=Φ6/12.5 cm in two orthogonal directions).

Table 3.2. The amount of longitudinal reinforcement.

Columns			Beams	
Frame		Reinforcement (%)	Maximum top reinforcement (%)	Maximum bottom reinforcement (%)
Y1	40/60 Φ40	1.4 2.4	0.5	0.3
Y2 and Y3	40/60 Φ40	1.0 1.3	1.8	1.1
Y4	40/60 Φ40	1.4 2.4	2.2	1.4
Y5	40/60 Φ40	2.1 3.0	1.8	1.4

After studying the given information about the RC frame-wall building some inferences were done; for instance, although the amount of longitudinal reinforcement, for some structural elements, is known the detailing of the reinforcement is not; therefore, it has been assumed as followed:

Table 3.3. Detailing of the longitudinal reinforcement.

COLUMNS			BEAMS	
Frame	Circular	Rectangular	Top reinforcement	Bottom reinforcement
Y1	15 bars #16	22 bars #14	5 bars #14	4 bars #12
Y2 & Y3	15 bars #12	16 bars #14	6 bars#20	6 bars #16
Y4	15 bars #16	22 bars #14	8 bars #20	8 bars#20
Y5	12 bars #20	16 bars #20	6 bars #20	5 bars#20

There is no information about the longitudinal reinforcement for beams in the X frames; then, reinforcement of beams in frames X1 and X4 is similar to that of frame Y1 and beams on frame X2 and X3 have equal amount of reinforcement as beams in frame Y3. It has to point out that although beams on frames Y1, X1 and X4 are analogous section dimensions are not. Also, It is noteworthy to mention that since the original configuration of the structure does not consider wall C, which was added to reduce torsional rotations by Kilar and Fajfar; then, that wall has not been taken into account for the present study.

The mechanical characteristics of the employed materials are presented in table 3.4. The concrete confinement factor K has been assumed equal to 1.1, this time, because there is lack of information about the transverse reinforcement.

Table 3.4. Material mechanical characteristics of the RC frame-wall building.

Unconfined concrete compression strength.	28 MPa.
Concrete strain at peak stress (Unconfined)	0.002
Steel yield strength for 12 mm bars	385 MPa
Steel maximum strength for 12 mm bars.	511 MPa
Maximum elongation at 5F baselength.	31.0%
Steel yield strength for 14 mm bars	434 MPa
Steel maximum strength for 14 mm bars.	559 MPa
Maximum elongation at 5F baselength.	29.0%
Steel yield strength for 16 mm bars	462 MPa
Steel maximum strength for 16 mm bars.	576 MPa
Maximum elongation at 5F baselength.	29.0%
Steel yield strength for 20 mm bars	462 MPa
Steel maximum strength for 20 mm bars.	576 MPa
Maximum elongation at 5F baselength.	29.0%

The concrete and longitudinal steel have been modeled by using the uniaxial constant confinement concrete model and the uniaxial Menegotto-Pinto steel model, respectively, previously used in the modeling of the SPEAR frame.

Idealization of the structure is based on linear elements placed at mid-depth of the members, and connected at the nodes. Main nodes are considered where column and beam elements meet, as it is showed in figure 3.11. Each member has been further subdivided in 3 or 4 elements to effectively

capture the expected inelasticity behavior, figure 3.12. As it was done for the SPEAR frame case, nodes located in the same column line share the last digits but the first digits change depending on the level where they belong. For instance, node 1 is located at the baseline, node 801, 1601, 2401 and 3201 are placed at first, second, third and fourth levels, respectively, sharing the same column line of number 1, see figure 3.11.

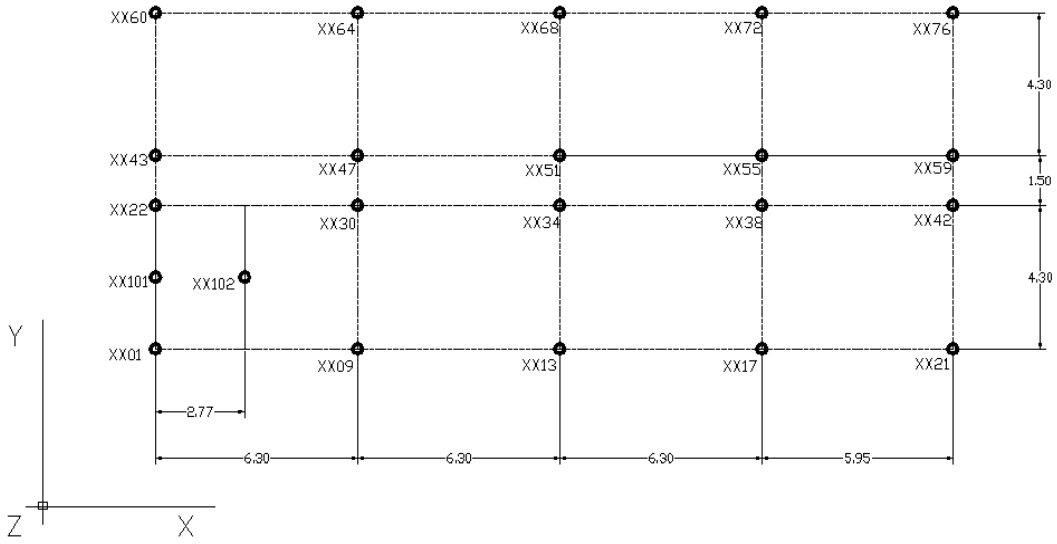

PLAN VIEW

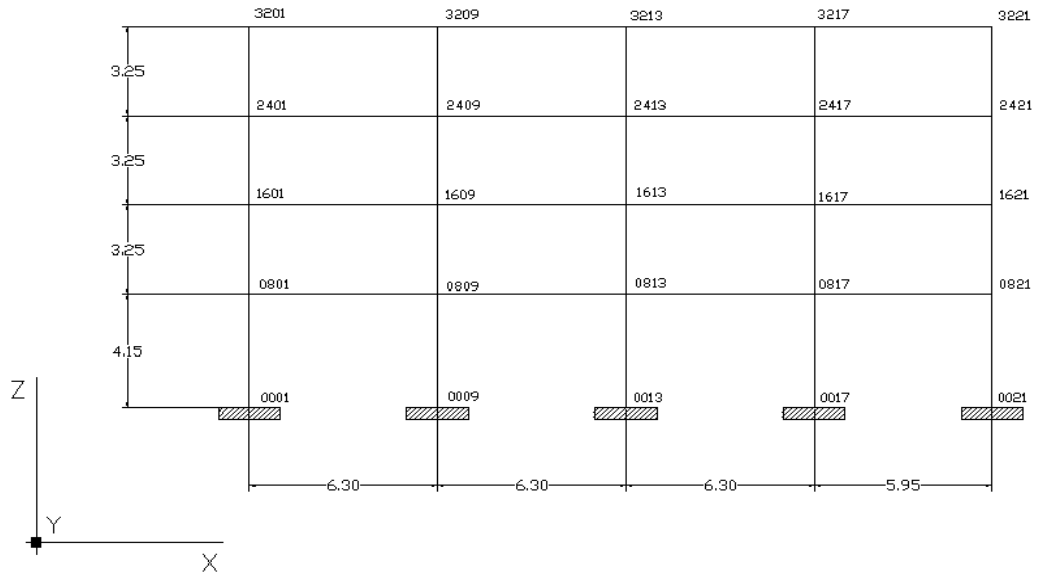

FRONTAL VIEW

Figure 3.11. System of coordinates and main node numbering.

The obtained information gives the total masses per storey and roof which amount 290 and 246 Ton, respectively; consequently, each level mass has been distributed among the main nodes, nodes where columns and beams meet. Gravity loads have been obtained from converting mass to loads and distributed them on the structural elements.

Structural member were modeled by employing distributed plasticity fiber element approach. Centerline dimensions of elements were used to account for additional deformations not modeled directly (bar slippage, yield penetration and shear joint distortion). The structural walls were idealized by using a RC flexural wall section model with a value of K equals to 1.2 in the fully confined areas. The walls were located at their centerlines and were connected to the adjacent nodes by rigid elements. Slabs were omitted in the analytical model since there is no information about that structural element; in addition, Kilar & Fajfar has not considered it in their analysis.

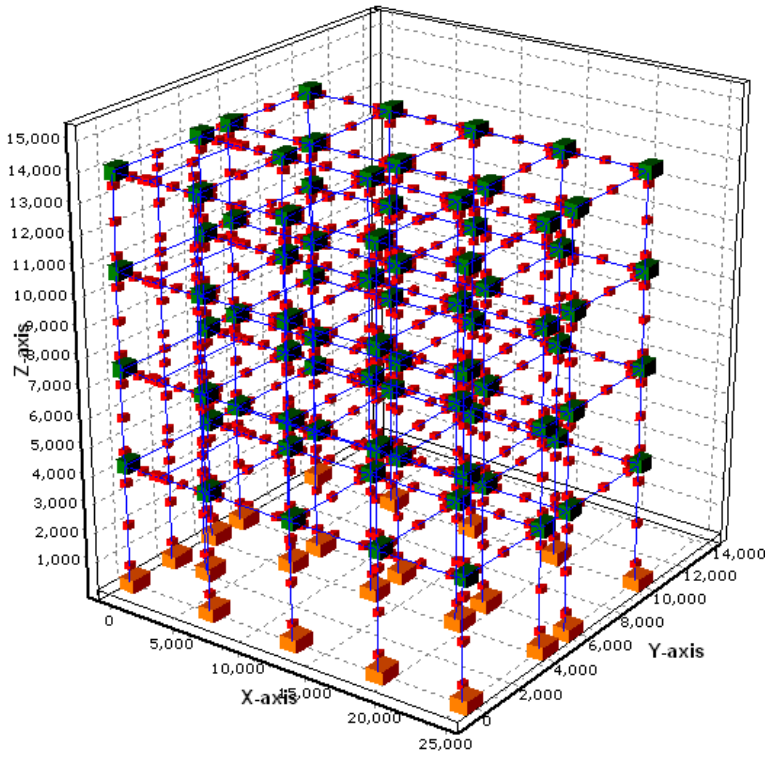

Figure 3.12. Final model of the RC frame-wall structure.

3.3 PERFORMED ANALYSES

3.3.1 The SPEAR model

Seismic response of the SPEAR structure was evaluated by three analysis procedures: Conventional static pushover, incremental dynamic analysis and adaptive pushover.

The conventional pushover was carried out by employing inverted triangular and uniform load patterns. The vertical load distribution, along the height of the building, is presented in table 3.5 for each load pattern. In addition, to account for the diaphragm action, the load for every level was further distributed at each main node according to the tributary mass per node, table 3.6. Each load pattern is applied in one horizontal direction only (either X or Y) and in two directions simultaneously. Thirty six pushover curves, the same number of interstory drift profiles, as well as ten shear profiles were obtained from the post processing of 12 conventional pushover analyses.

Table 3.5. Vertical load distribution per load pattern.

Floor	Mass (T)	Triangular pattern. Force (kN)	Uniform pattern. Force (kN)
First	59.865	86.359	172.718
Second	59.865	172.718	172.718
Roof	59.865	259.077	172.718
Sum	179.595	Total base shear = 518.153	Total base shear = 518.153

Table 3.6. Percentage of the load distribution in plan base on the tributary mass per main node.

Main node in plan	Area (m^2)	% of Total Area
XX23	4.125	4.188
XX27	11.000	11.168
XX31	12.600	12.792
XX12	7.875	7.995
XX17	22.000	22.335
XX21	14.000	14.213
XX22	6.000	6.091
XX01	3.750	3.807
XX06	9.750	9.898
XX11	7.400	7.513
Sum	98.5	100.000

Incremental dynamic analysis was performed by using six ground motion records. The records were selected based on the criteria of magnitude (M), peak ground acceleration (PGA) and the shape of the accelerograms (it was decided that selected records should not show single pulses of high acceleration). The ratio between the two horizontal components was not altered. Both horizontal components were applied simultaneously. It is noteworthy that the stronger component was applied in the strong direction of the building, the Y direction in this case. The basic characteristics of the ground motions are presented in table 3.7 and the elastic response spectra are shown in figures 3.13 and 3.14. Additionally, the stronger component of each ground motion was scaled to five different PGA values (0.1g, 0.2g, 0.3g, 0.4g and 0.5g). Sixty incremental dynamic analyses produced 360 sets of response points, equal number of interstory drifts and 60 shear profiles.

Table 3.7. Characteristics of the selected earthquakes.

Earthquake name	Date	Station
Imperial Valley	18 May 1940	El Centro site Imperial Valley irrigation district.
Friuli	06 May 1976	Tolmezzo-Diga Ambiesta.
Kalamata	13 Sep 1986	Kalamata-Prefecture.
Loma Prieta	17 Oct 1989	Capitolia-Fire Station.
Loma Prieta	17 Oct 1989	Emeryville.
Northridge	17 Jan 1994	Arleta-Nordhoff Ave. Fire Station.

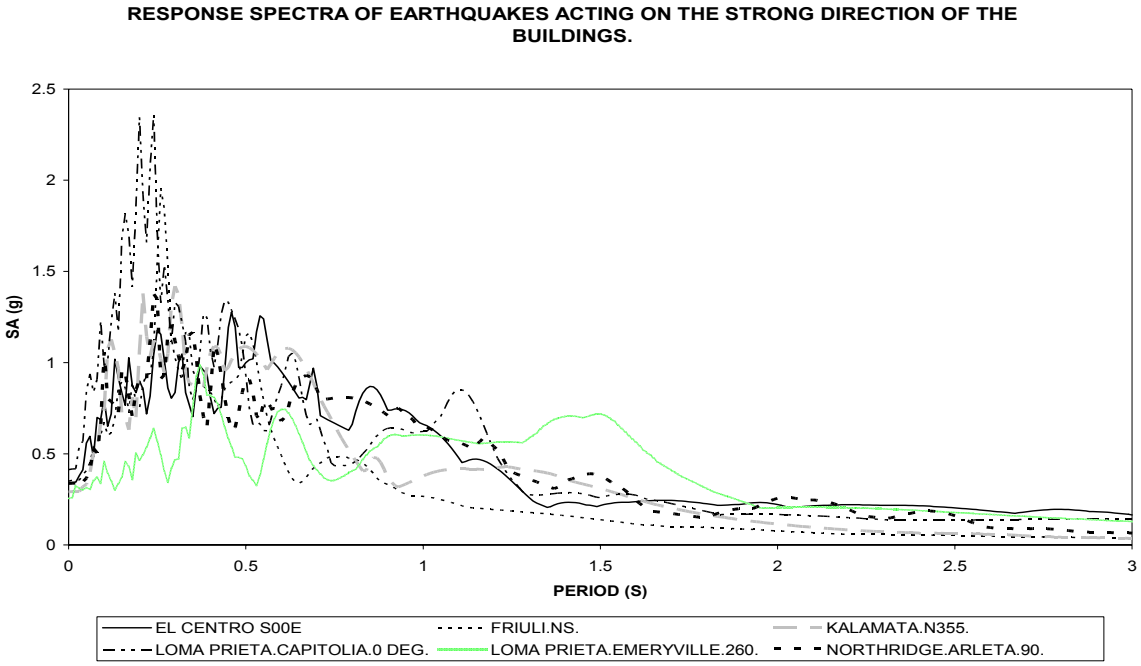

Figure 3.13. Response spectra of earthquakes acting along the strong direction.

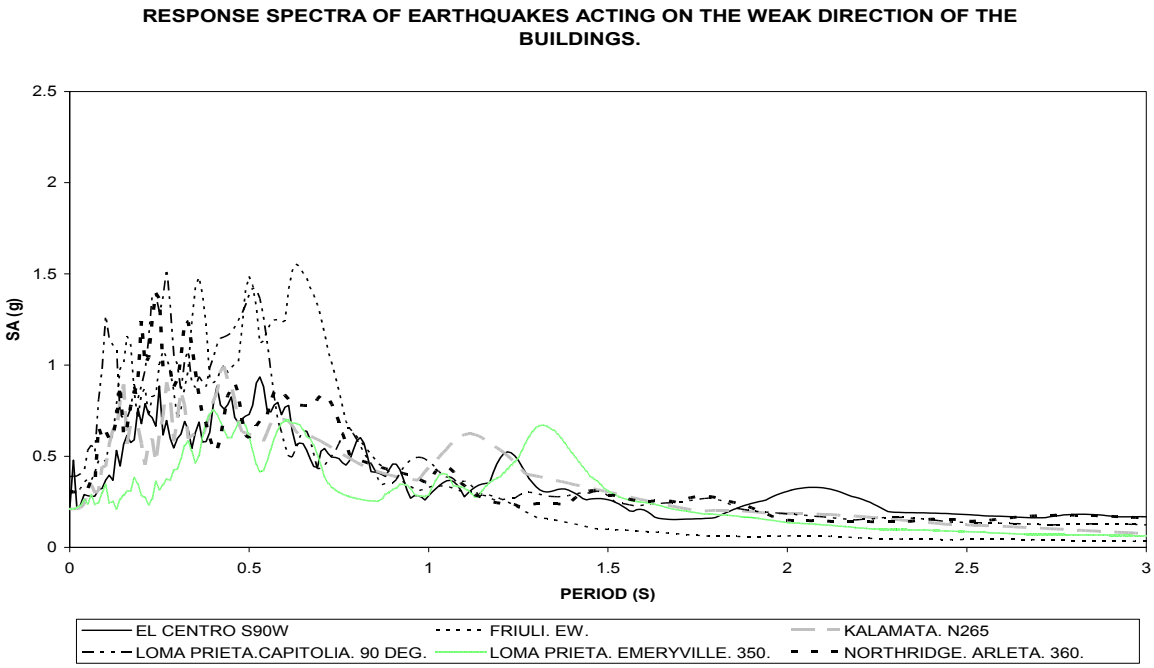

Figure 3.14. Response spectra of earthquakes acting along the weak direction.

The two variants of the adaptive pushover method were used Force-based (FAP) and Displacement-based (DAP). Loads were applied in one direction only (either X or Y) and in the two direction simultaneously. Loads were located at the intersection between columns and beams, or main nodes. Different from the conventional pushover, the initial load distribution, both in elevation and plan, is uniform. Thirty six pushover curves, equal number of interstory drift profiles, as well as ten shear profiles were obtained from the post processing of 12 conventional pushover analyses.

Force-based adaptive pushover was using by applying an initial force of 10000 N at all main nodes. A force-based scaling, where modal forces distributions are used for scaling, was employed; similarly, incremental updating, as a mean to increment the forces and update their distribution, was utilized. In addition, since the structure is asymmetric pushovers in the negative direction were also computed. The loading/solution scheme utilized was adaptive load control plus automatic response control, meaning that the analysis starts using adaptive load control; then, once the program, for any reason, is not able to continue applying loads changes to automatic response control.

Likewise, to execute the displacement-based pushover (DAP) an initial displacement of 300 mm, applied at all main nodes, was employed. The scheme followed to run the DAP analyses was similar to that of the FAP noting that displacement-based scaling, instead of force-based scaling, was employed.

3.3.2 The RC Frame-wall model

Seismic response of the RC frame-wall structure was evaluated by the same three analysis procedures used above: Conventional static pushover, incremental dynamic analysis and adaptive pushover.

The conventional pushover was carried out by employing inverted triangular and uniform load patterns. The vertical load distribution, along the height of the building, is presented in table 3.8 for each load pattern. In addition, to account for the diaphragm action, the load for every level was further distributed at each main node according to the tributary mass per node, table 3.9. Each load pattern is applied in one horizontal direction only (either X or Y) and in two directions simultaneously. Thirty six pushover curves, the same number of interstory drift profiles, as well as ten shear profiles were obtained from the post processing of 12 conventional pushover analyses.

Table 3.8. Vertical load distribution per load pattern.

Floor	Mass (T)	Triangular pattern. Force (kN)	Uniform pattern. Force (kN)
First	290.00	393.11	804.9475
Second	290.00	700.96	804.9475
Third	290.00	1008.82	804.9475
Roof	246.00	1116.90	804.9475
Sum	1116.00	Total base shear = 3219.79	Total base shear = 3219.79

Table 3.9. Percentage of the load distribution in plan base on the tributary mass per main node.

Main node in plan	Area (m^2)	% of Total Area
XX01	6.7725	2.70
XX09	13.545	5.40
XX13	13.545	5.40
XX17	13.16875	5.25
XX21	6.39625	2.55
XX22	9.135	3.64
XX30	18.27	7.28
XX34	18.27	7.28
XX38	17.7625	7.08
XX42	8.6275	3.44
XX43	9.135	3.64
XX47	18.27	7.28
XX51	18.27	7.28
XX55	17.7625	7.08
XX59	8.6275	3.44
XX60	6.7725	2.70
XX64	13.545	5.40
XX68	13.545	5.40
XX72	13.16875	5.25
XX76	6.39625	2.55
Sum	250.985	100.00

Incremental dynamic analysis was performed by using a similar scheme used for the SPEAR model with six ground motion records. The basic characteristics of the ground motions are presented in table 3.4 and the elastic response spectra are shown in figures 3.9 and 3.10. Sixty incremental dynamic analyses produced 360 sets of response points, equal number of interstory drifts and 60 shear profiles.

Adaptive pushover procedure for RC frame-wall model was similar to that of the SPEAR model, except that initial uniform load was set up to 30000 N, for the Force-based scheme, and to 1000 mm, for the Displacement-based method.

4. CASE STUDIES

4.1 INTRODUCTION

In the following section, a summary of the analysis carried out on the two models presented above is shown. The most important results are exhibited and some remarks are drawn. Outcomes from pushover, dynamic and adaptive pushover analysis are shown. Some general considerations, regarding the force or action application, have to bear in mind; for instance, the direction of the application of forces in the pushover case

4.2 DYNAMIC CHARACTERISTICS

4.2.1. SPEAR model

The elastic periods of vibration and the corresponding deform shapes are computed to assess the model reliability. All shapes show displacement components in the three directions; however, first and second modes of vibration have predominant X and Y translation components, respectively. The third mode has an important torsional component on the Z direction. Table 4.1 presents the first four period of vibrations and figure 4.1 show the deform shapes related to those periods.

Table 4.1. First four periods of vibration of SPEAR frame model.

Mode	1	2	3	4
T (s)	0.688	0.597	0.491	0.239

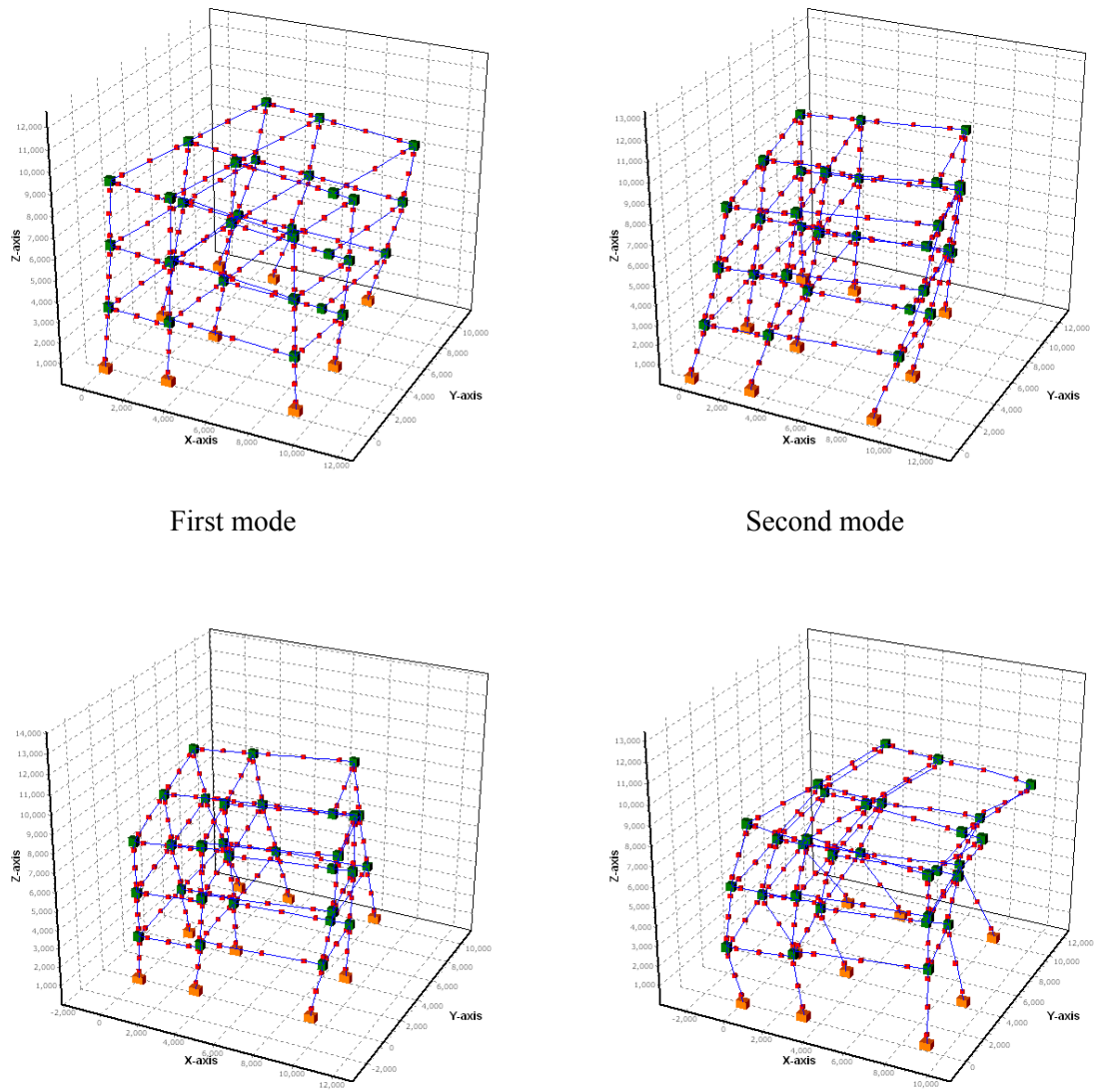

First mode Second mode

Third mode Fourth mode

Figure 4.1. First four deform shapes of the SPEAR frame model.

4.2.2. RC frame-wall model

The elastic periods of vibration and the corresponding deform shapes have been computed. The first four period of vibrations and the deform shapes related to those periods are presented en table 4.2 and figure 4.66, respectively. The first mode portrays a predominant deform shape on the X direction, along the long axis of the building. The second mode displays torsion around the shear walls located at one extreme of the structure, the stiff edge, which, in turn, creates deformation on the Y direction at the flexible edge.

Table 4.2. First four periods of vibration of the RC frame-wall model.

Mode	1	2	3	4
T (s)	0.920	0.843	0.522	0.437

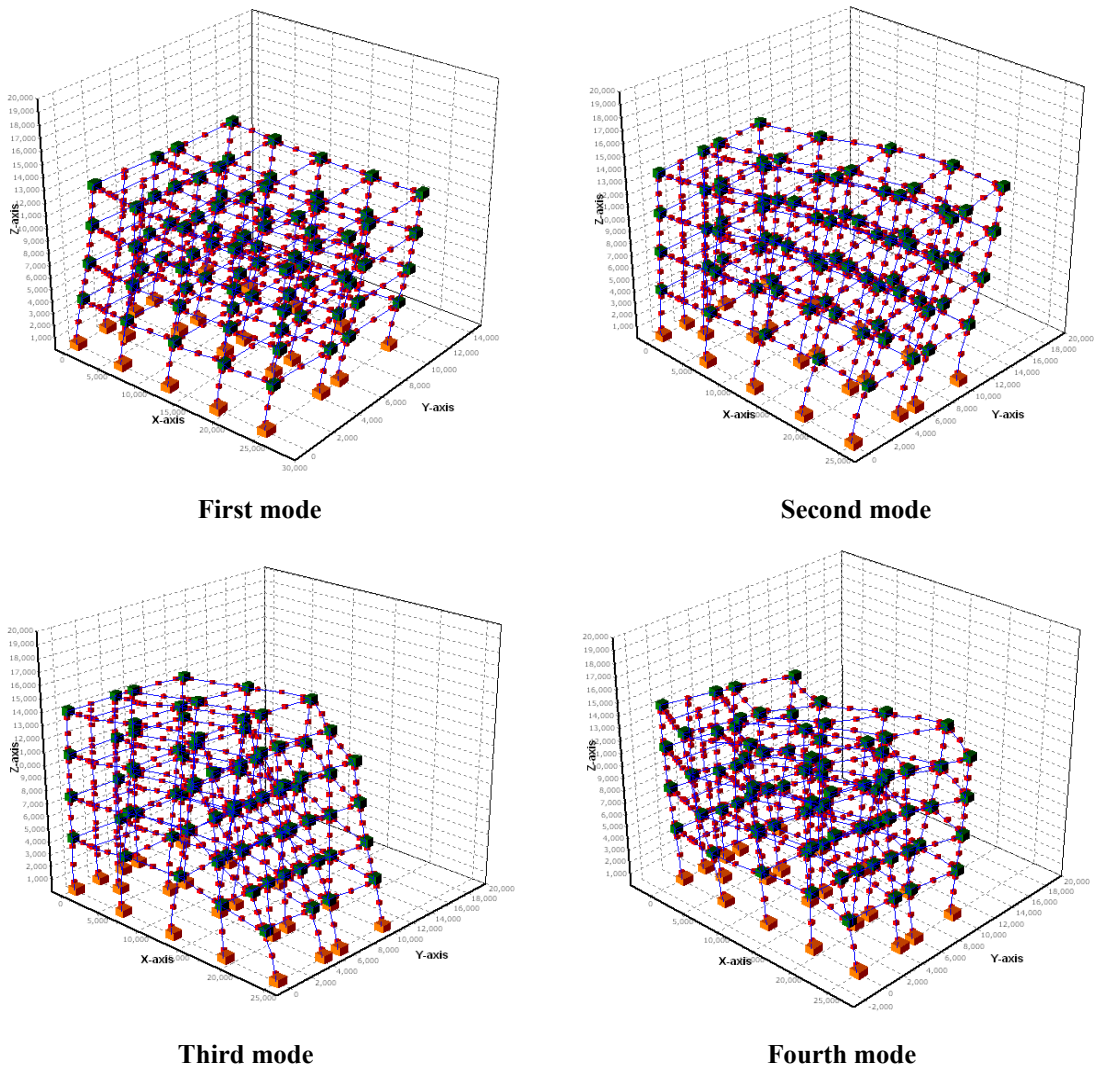

First mode **Second mode**

Third mode **Fourth mode**

Figure 4.2. First four deform shapes of the RC frame-wall model.

4.3. RESULTS

4.3.1. Diaphragm effects

The in-plan behavior of the floor diaphragm has been the first issue to be considered. It has been shown by others [e.g. Duoduomis & Athanatopoulou, 2001] that the rigid floor diaphragm concept becomes questionable when the shape of the floor plan is very elongated or does not have a regular shape. That study states that the stresses of the frame members of a structure (columns, beams, walls) depend only on the displacements at the nodal points where they are connected to the diaphragm;

therefore, a mean to describe the in-plane displacement of the diaphragm must be found. Two dimensional finite elements were used to model the diaphragm effects.

In the present research, the SPEAR model was tested to assess the slab effects. In-plan behavior of the floor diaphragm has been modeled by employing braces. Following a methodology presented by P. Franchin, M. Schotanus and P Pinto [2003], braces have an area of 0.1 the length of the diagonal, as the width, by the thickness of the slab, as the height. Five different arrangement were tried: No bracing; bracing with the elastic modulus of the concrete and preventing rotation at the extreme of braces, named as “braces”; bracing with the modulus of elasticity equals to 1e12 MPa and rotation prevented at the element extremes, called as “stiff braces”; braces with similar characteristics to the second case but rotation are allowed, called “braces-pin”; and braces with elastic stiffness equal to 1e12 MPa with allowed rotation at the ends, named as “stiff braces-pin”. Figures 4.3 and 4.4 illustrate the strength of the system in the weak and strong directions, respectively.

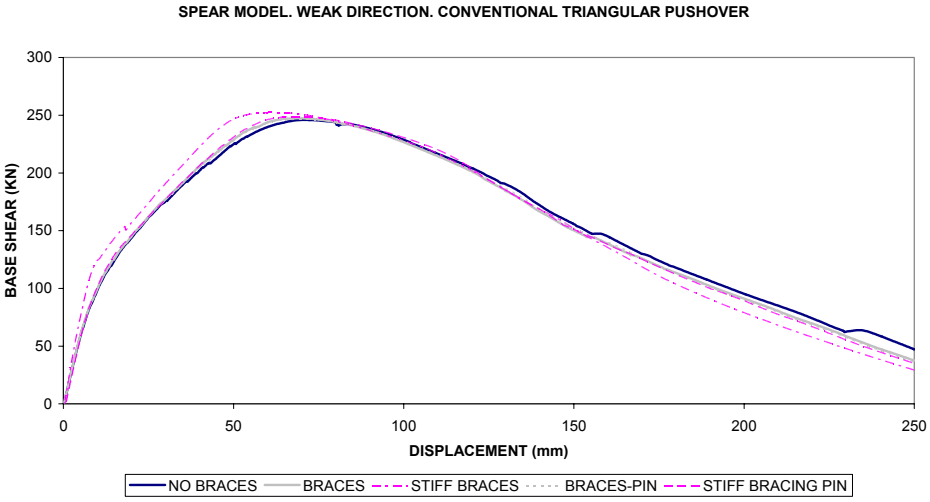

Figure 4.3. Pushover curve of the weak direction.

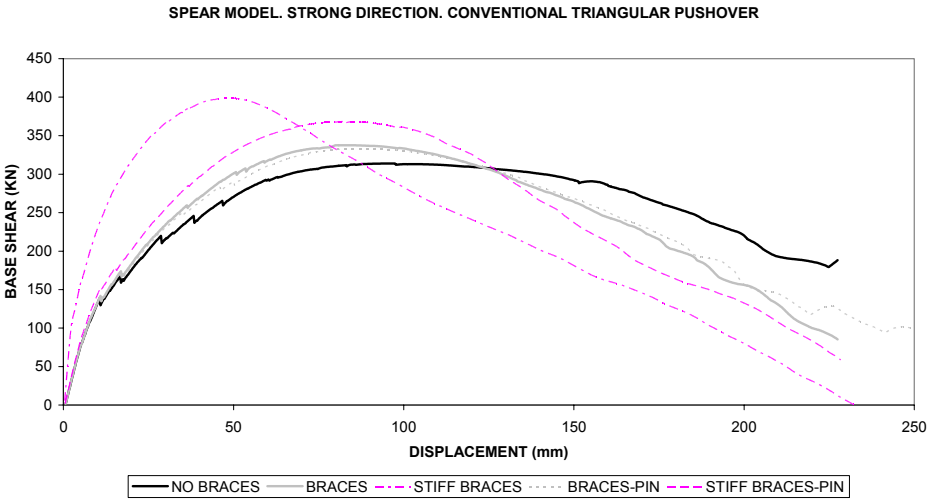

Figure 4.4. Pushover curve of the strong direction.

Contrary to what happen in the weak axis, where the predicted pushover curves do not show great variation, the strong direction portrays remarkable strength differences depending on the type of bracing configuration. This outcome may be produced due to differences in strength and stiffness of the resisting elements that mainly affect that direction. The plots clearly highlight the importance of the bracing characteristics employed to account for the diaphragm action. At this stage of the present study is not clear which is the best option of all; therefore, models have been considered with no bracing. Further studies will be carried out to elucidate the appropriate model to include the in-plan behavior of floor diaphragms by using either plate, shell or solid elements.

4.3.2. Incremental dynamic analysis.

A comparison between the pushover analysis and the incremental dynamic analysis must be done in order to validate the results from the former. Matching capacity curves (top displacement vs. base shear) against time history results is one of the processes that is usually performed. However, the pairing dynamic base shear-displacement can be done in various ways such as: maximum base shear – maximum displacement, independent of the time of occurrence; maximum displacement – corresponding base shear, using a time window of 0.5s; and absolute maximum base shear – corresponding displacement, again using a 0.5s time frame. Comparison between the three different ways of pairing the dynamic results from all ground motions and the conventional triangular pushover, using the two models, are portrayed in figures 4.5 to 4.8.

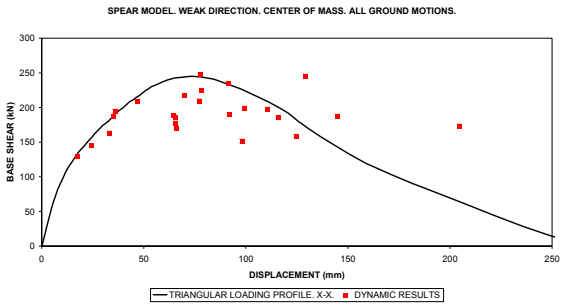

Maximum displacement vs. maximum base shear.

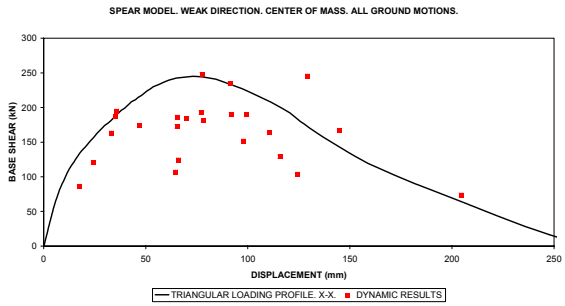

Maximum displacement vs. "corresponding" base shear.

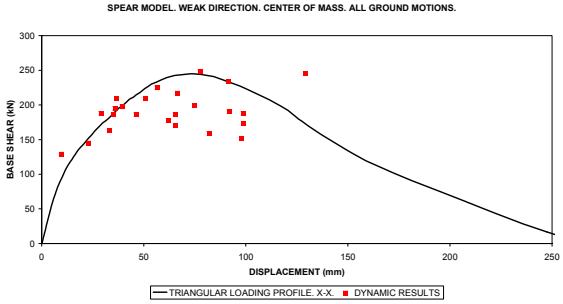

Maximum base shear vs. "corresponding" displacement.

Figure 4.5. Conventional triangular pushover compared to time histories results employing three different arrangements. SPEAR model. Weak direction. Center of mass.

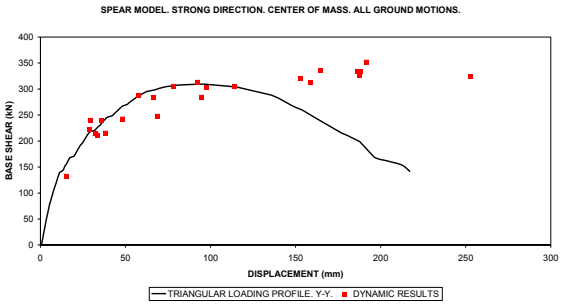

Maximum displacement vs. maximum base shear.

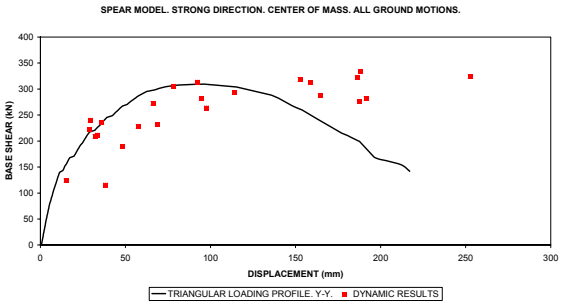

Maximum displacement vs. "corresponding" base shear.

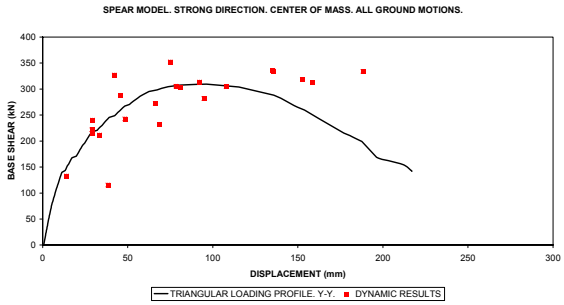

Maximum base shear vs. "corresponding" displacement.

Figure 4.6. Conventional triangular pushover compared to time histories results employing three different arrangements. SPEAR model. Strong direction. Center of mass.

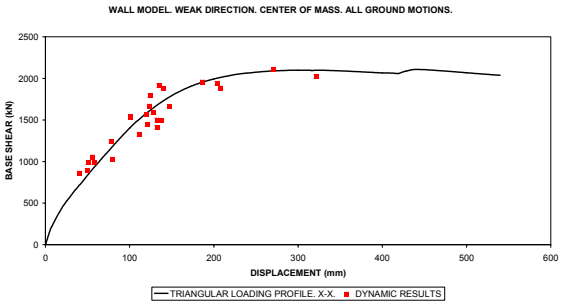

Maximum displacement vs. maximum base shear.

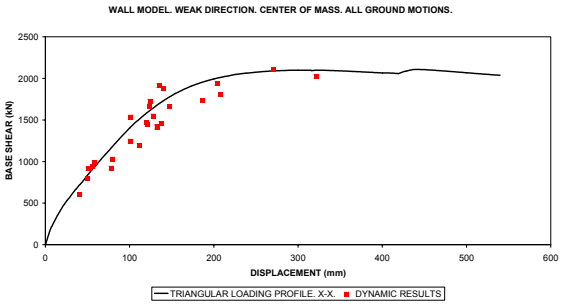

Maximum displacement vs. "corresponding" base shear.

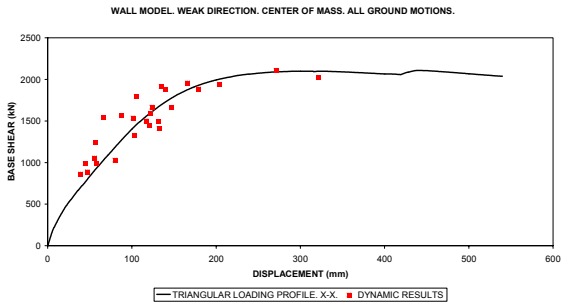

Maximum base shear vs. "corresponding" displacement.

Figure 4.7. Conventional triangular pushover compared to time histories results employing three different arrangements. RC frame-wall model. Weak direction. Center of mass.

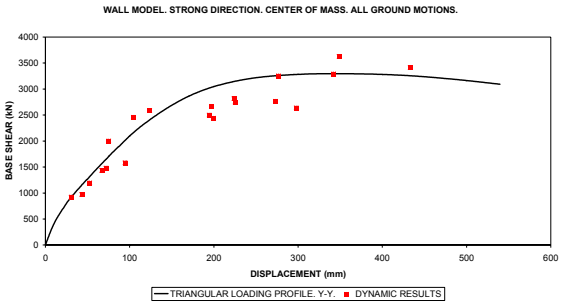

Maximum displacement vs. maximum base shear.

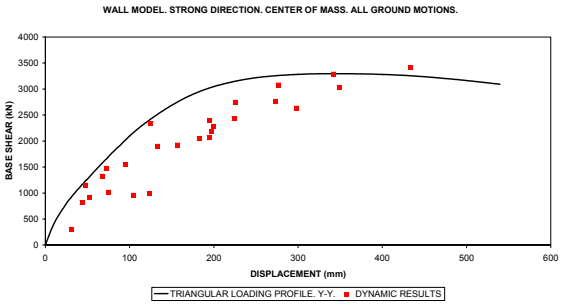

Maximum displacement vs. "corresponding" base shear.

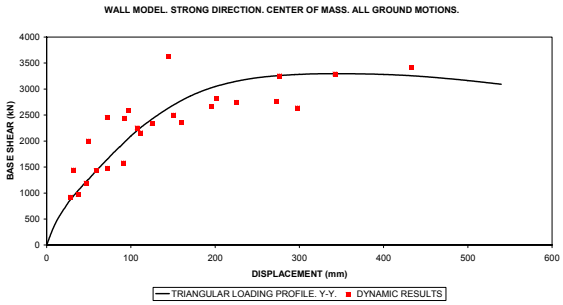

Maximum base shear vs. "corresponding" displacement.

Figure 4.8. Conventional triangular pushover compared to time histories results employing three different arrangements. RC frame-wall model. Strong direction. Center of mass.

Spear model. It is seen that in the strong direction the arrangement maximum base shear against "corresponding" displacement is the one that close matches the conventional pushover however the fitting is not entirely satisfactory. The correlation in the weak direction is even less clear but the maximum base shear versus "corresponding" displacement arrangement still provides acceptable fitting between dynamic and static results.

Wall model. If the weak direction is studied, it seems that all arrangements produce good correlation to the static plots. The matching in the strong direction is less clear but still the maximum base shear versus "corresponding" displacement arrangement gives the best fitting between dynamic and static results

From the analysis of two models, by employing three selected points, two directions and two loading profiles for each building, it is not clear which is the best alternative; however, the combination maximum base shear with corresponding displacement seems to have a small advantage and thus will be adopted in all subsequent plots.

4.3.3 Direction of loading application.

In this section the results of pushovers applying forces in one direction and in two directions simultaneously are shown. These plots are matched with the dynamic results of one ground motion depending on the case; for instance, Northridge earthquake is used for the SPEAR model and Capitolia is used in the RC frame-wall building. Only one earthquake, for each structure, has been used because the scatter is less and the relationships are easier to see; but the outcome is still valid for other ground motions since this process was done by using all dynamic results altogether. It has to be remembered that the arrangement maximum base shear vs. corresponding displacement has been used to plot the dynamic response points.

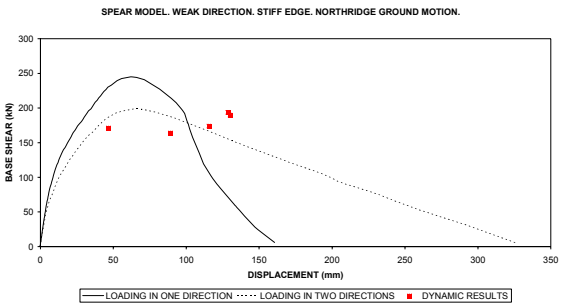

Stiff edge.

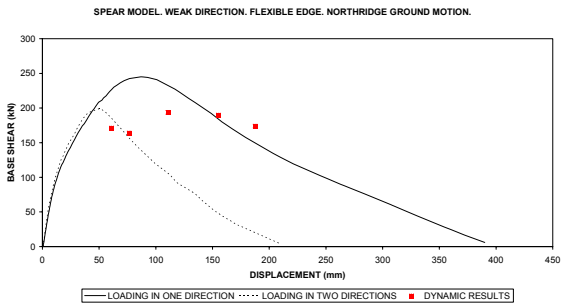

Flexible edge.

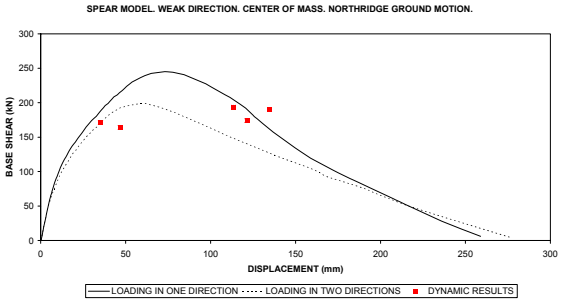

Center of mass.

Figure 4.9. Triangular conventional pushover versus dynamic results from the Northridge record. Weak direction. SPEAR model.

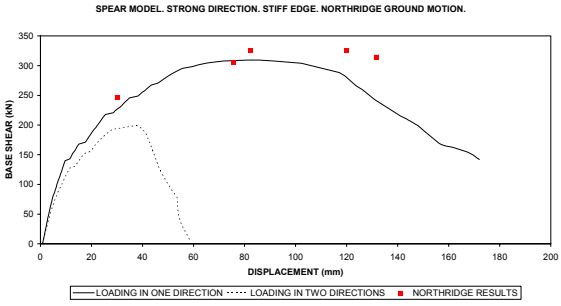

Stiff edge.

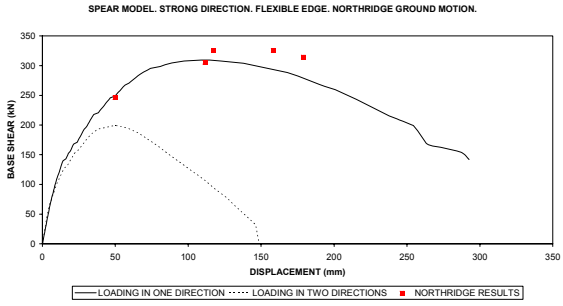

Flexible edge.

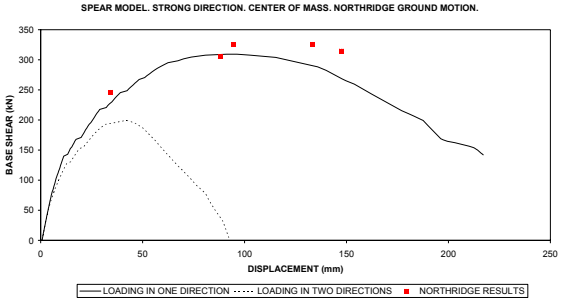

Center of mass.

Figure 4.10. Triangular conventional pushover versus dynamic results from the Northridge record. Strong direction. SPEAR model.

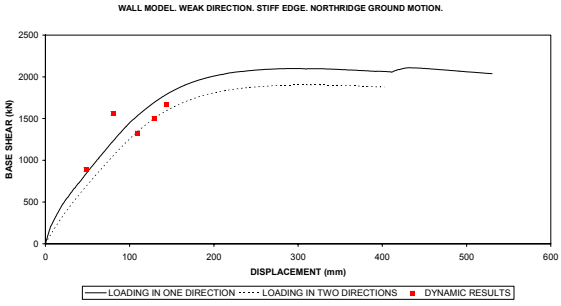

Stiff edge.

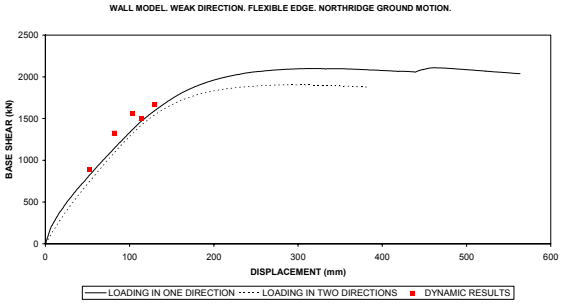

Flexible edge.

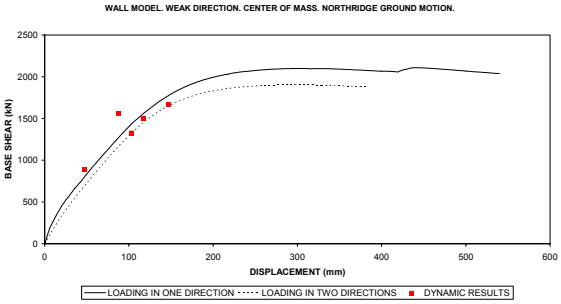

Center of mass.

Figure 4.11. Triangular conventional pushover versus dynamic results from the Capitolia record. Weak direction. RC frame-wall model.

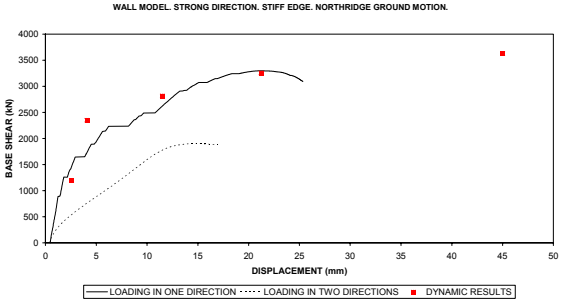

Stiff edge.

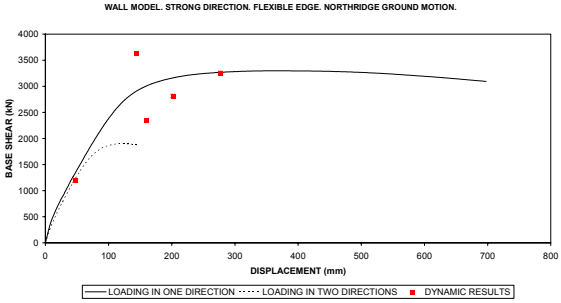

Flexible edge.

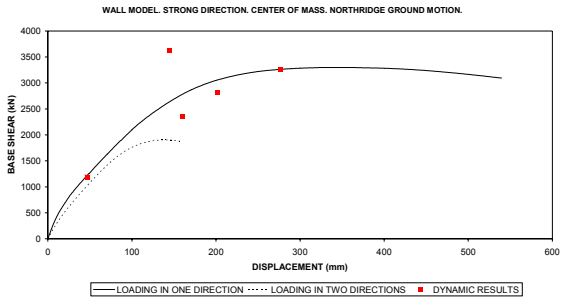

Center of mass.

Figure 4.12. Triangular conventional pushover versus dynamic results from the Capitolia record. Strong direction. RC frame-wall model

Spear model. There are clear differences from pushing in a single direction or in both at the same time, trend which is more noticeable in the strong direction. In general, pushing in one direction predicts higher values of strength and agrees better with the dynamic results, except at the stiff edge in the weak direction where there is not a clear tendency.

Wall model. The most striking observation from the figures above is that pushing in one direction or in both at the same time makes little difference when the weak direction is studied, figure 4.11. The dynamic outcomes agree very well with the static ones and they lie along the both pushover curves; such agreement is not observed when the strong direction is analyzed. It is clear that pushing in both directions under predict the dynamic response while applying forces in one axis gives answers that better agree with the time history analysis. A possible explanation for the observed trend might be that the structural system along the weak direction is composed by frames, which might produces comparable responses from static and dynamic analyses. On the other hand, the structural walls along the strong direction, and positioned at one corner of the building, make the bidirectional pushover fails to capture the response of the structure in that direction.

It is apparent, from the above figures, that applying loads in one direction is the alternative that better matches the dynamic results. The above state is well confirmed in the strong direction of both structures and in lesser degree in the weak direction. It has to be pointed out that the worst point to match is the stiff edge, in almost all cases.

It should be noticed that in this research the possibility of applying the same component, of an earthquake, to both directions of a model has not been explored. This procedure could produce dynamic outcomes that might match the pushover results when static load is applied in both directions, simultaneously.

4.3.4 Loading profile for conventional pushover

Two types of loading profiles were compared, triangular and uniform. Again the two structures, two directions for each model and three selected points are used to draw a conclusion. Figures 4.13 to 4.16 show the pushover curves versus the dynamic results.

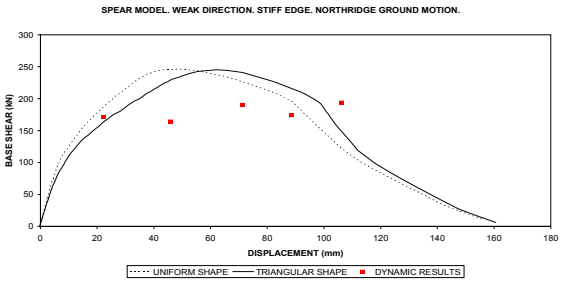

Stiff edge.

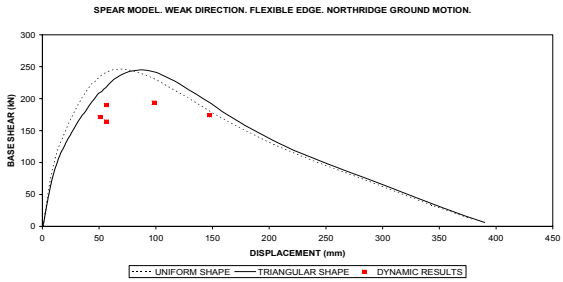

Flexible edge.

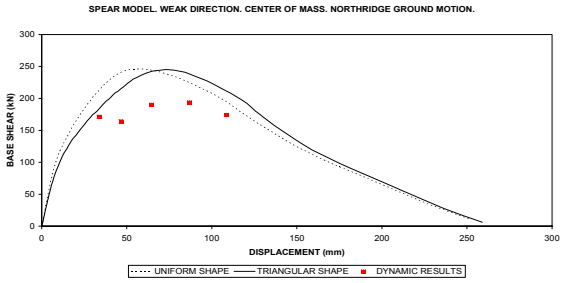

Center of mass.

Figure 4.13. Triangular and uniform conventional pushovers versus dynamic results. Weak direction. SPEAR model.

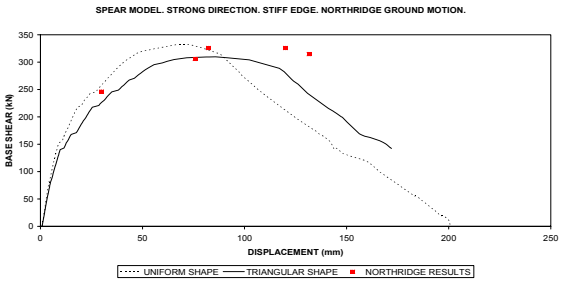

Stiff edge.

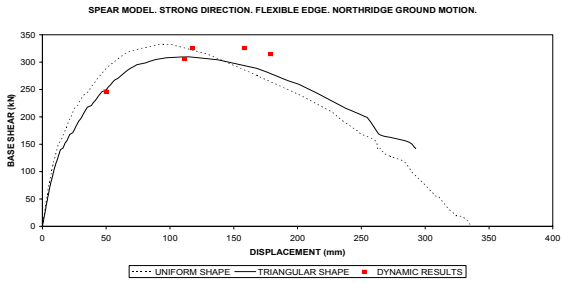

Flexible edge.

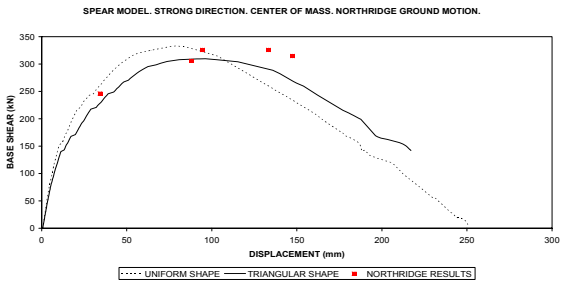

Center of mass.

Figure 4.14. Triangular and uniform conventional pushovers versus dynamic results. Strong direction. SPEAR model.

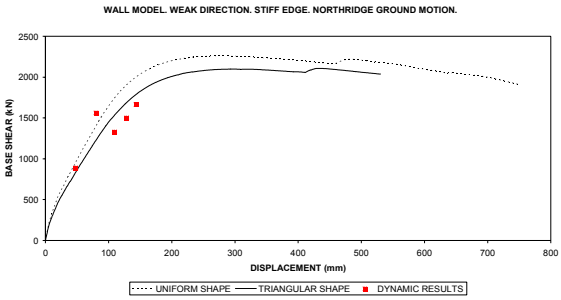

Stiff edge.

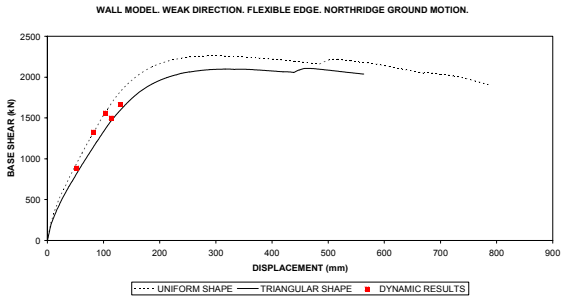

Flexible edge.

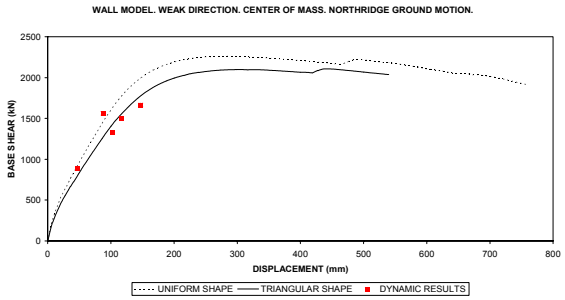

Center of mass.

Figure 4.15. Triangular and uniform conventional pushovers versus dynamic results. Weak direction. RC frame-wall model.

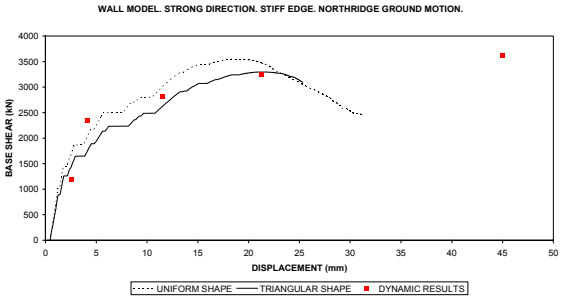

Stiff edge.

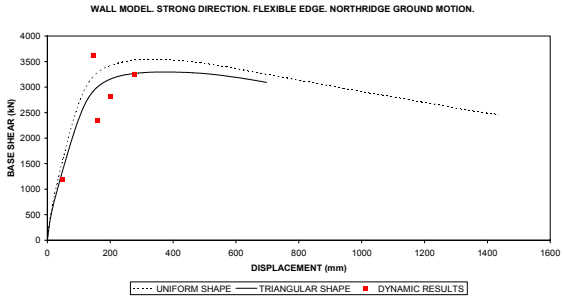

Flexible edge.

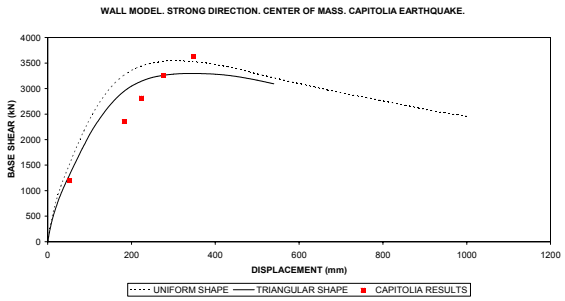

Center of mass.

Figure 4.16. Triangular and uniform conventional pushovers versus dynamic results. Strong direction. RC frame-wall model.

From the figures above, it seems that triangular loading profile better matches the dynamic points for both models; however, the wall model may create some doubts about the precedent statement; therefore, interstory drifts profiles will be compared next. The subsequent figures show the drift

profiles of center of mass, for both models; but the processed data has included the analysis of both stiff and flexible edges.

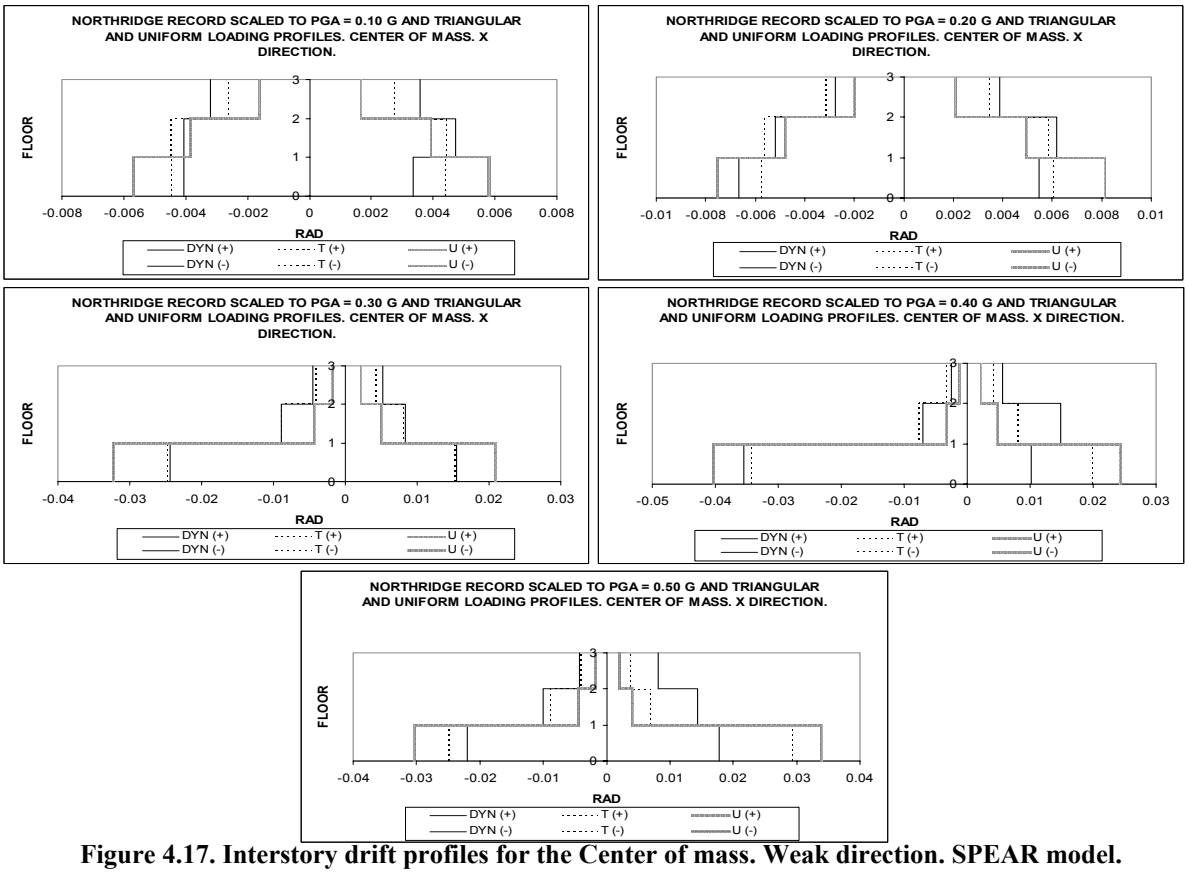

Figure 4.17. Interstory drift profiles for the Center of mass. Weak direction. SPEAR model.

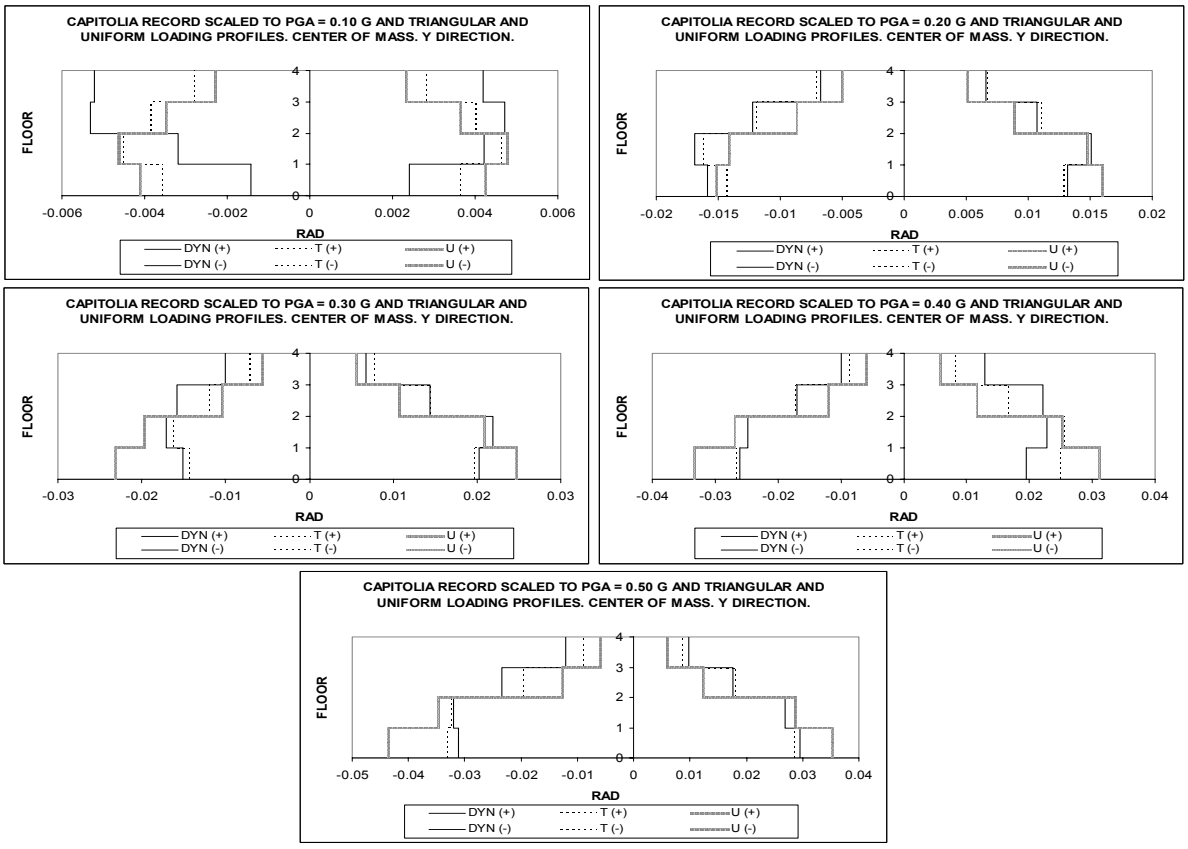

Figure 4.18. Interstory drift profiles for the Center of mass. Strong direction. SPEAR model.

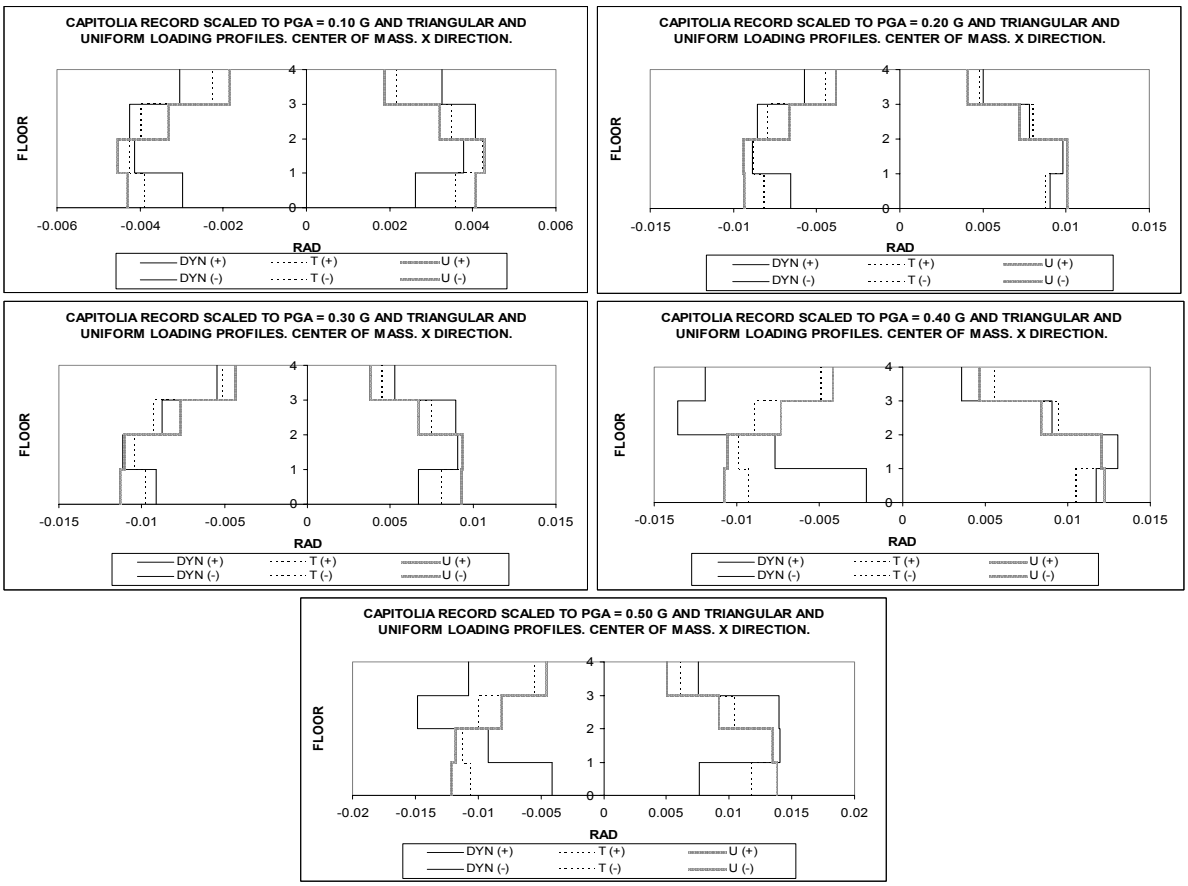

Figure 4.19. Interstory drift profiles for the Center of mass. Weak direction. RC frame-wall model.

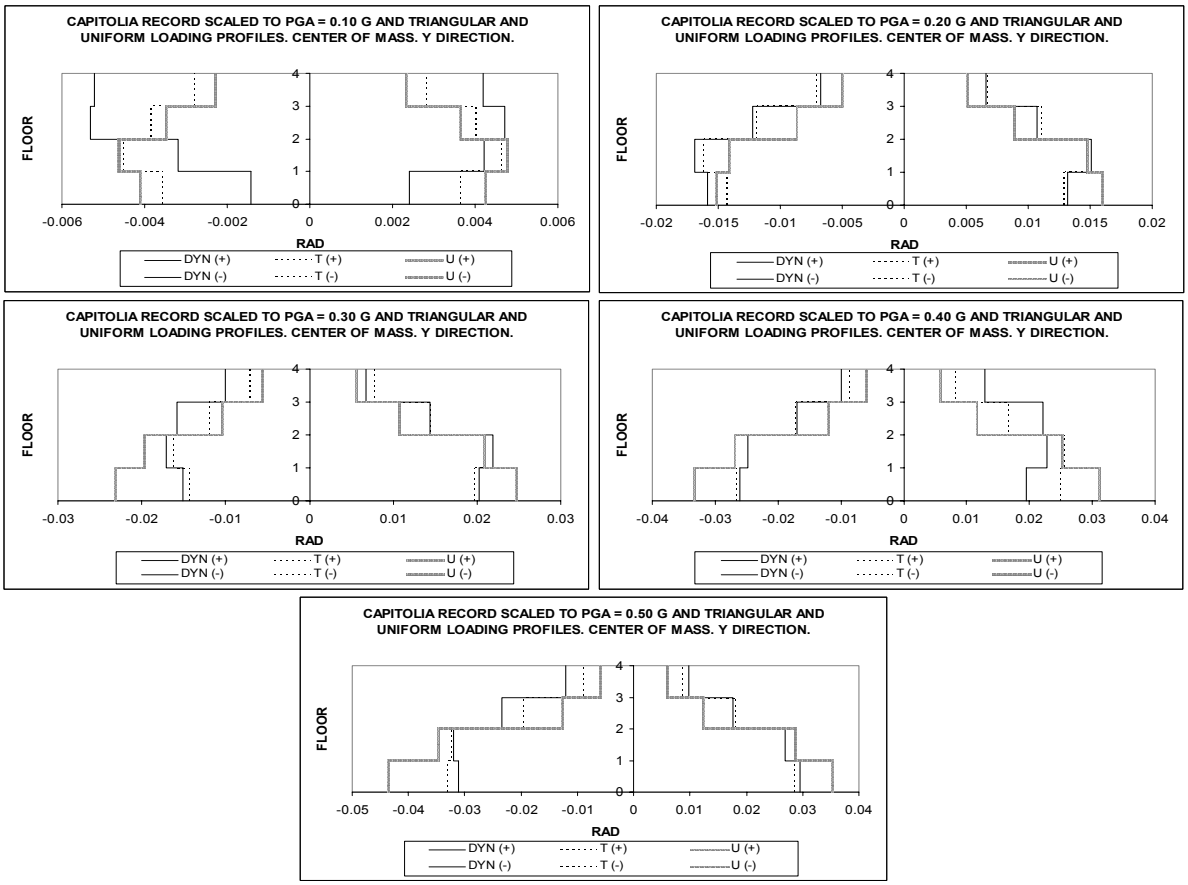

Figure 4.20. Interstory drift profiles for the Center of mass. Strong direction. RC frame-wall model.

Spear model. The triangular loading shape is more suitable to represent the dynamic interstory drift profiles than its static counterpart; for instance, there is remarkable agreement at the strong direction in all selected nodes (center of mass, stiff edge and flexible edge). However, at the weak direction matching is not very impressive and in many cases it fails to represent the interstory drift obtained by time history analysis.

Wall model. It is clear that the triangular profile is more suitable to represent the dynamic interstory drift profiles than its static counterpart; for instance, there is remarkable agreement at the flexible edge in both directions; good accord at the center of mass in the strong direction and some levels of intensities in the weak direction; and at the stiff edge in the positive weak direction mainly, but, at the perpendicular direction there is no match, except for very low levels of intensities

In general, the interstory drift profiles obtained from the triangular loading distribution better represents the dynamic drift profiles. At high PGA levels none of the two static loading distributions seems to work well. Nevertheless, the triangular distribution appears to be the correct option for the two considered models. The end result is that in the case of conventional static pushover the best selection is an analysis using a triangular loading distribution, pushing the structure in one direction.

4.3.5 Adaptive pushover scheme

It has been mentioned before that there are two methods in the adaptive pushover, force-based (FAP) and displacement-based (DAP). Next, the appropriated adaptive scheme will be chosen base on the comparison between capacity curves and the dynamic results; as well as, on the interstory drift profiles. Figures 4.21 to 4.24 display the adaptive pushover curves compared to the dynamic response points and figures 4.25 to 4.28 portray the matching of interstory drift profiles at the center of mass for both models. Northridge record and Capitolia ground motion will be used for the SPEAR and RC frame-wall models, respectively. In addition, adaptive pushover with loads applied unidirectionally will be employed, based on results of a similar work as the one performed for the conventional pushover.

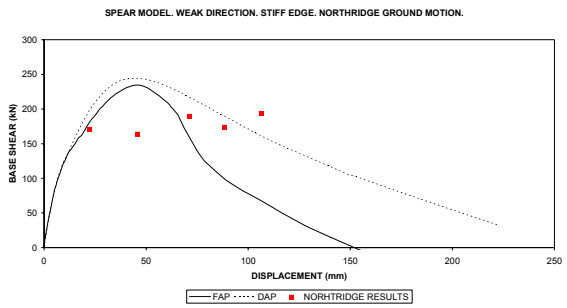

Stiff edge.

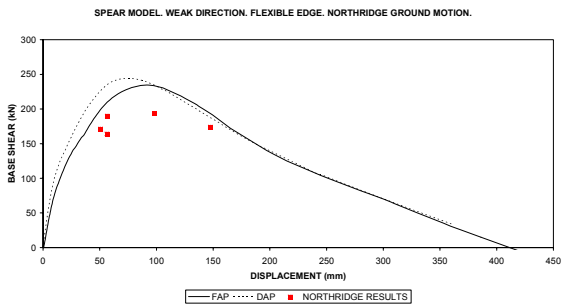

Flexible edge.

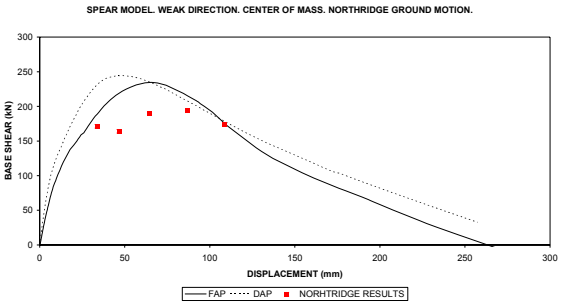

Center of mass

Figure 4.21. FAP and DAP versus Northridge results. Weak direction. SPEAR model.

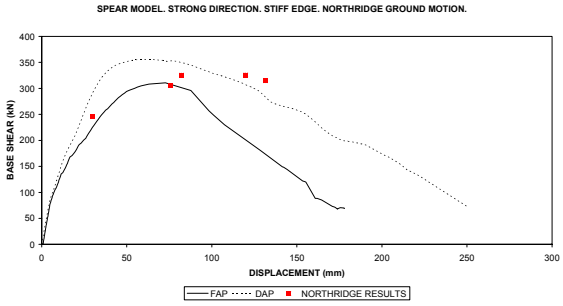

Stiff edge.

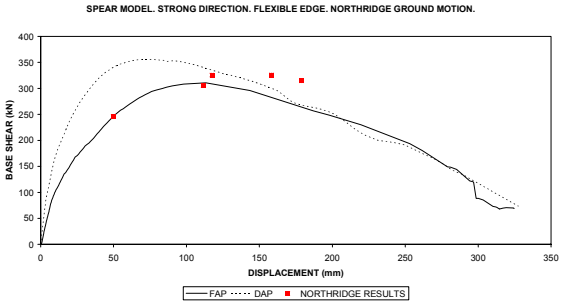

Flexible edge.

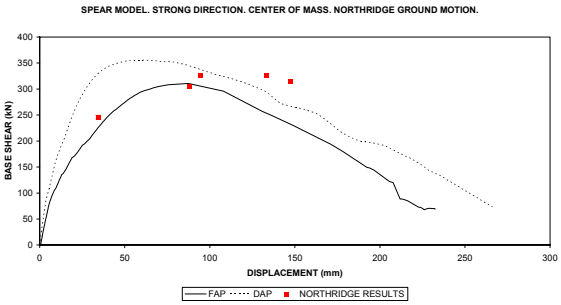

Center of mass

Figure 4.22. FAP and DAP versus Northridge results. Strong direction. SPEAR model.

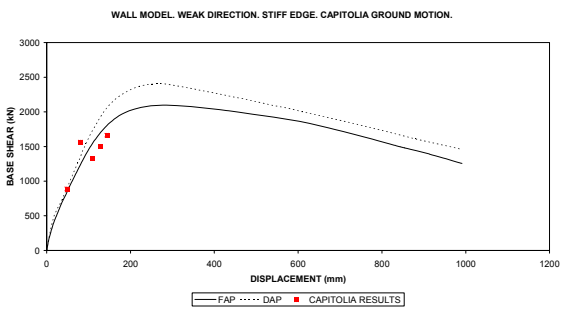

Stiff edge.

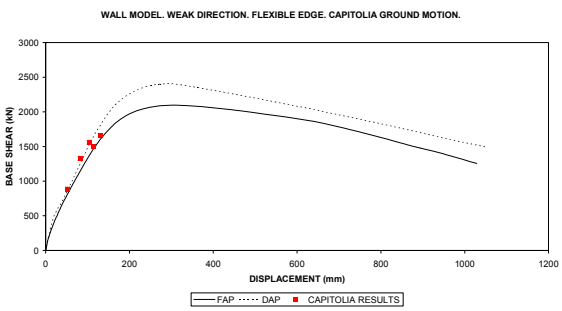

Flexible edge.

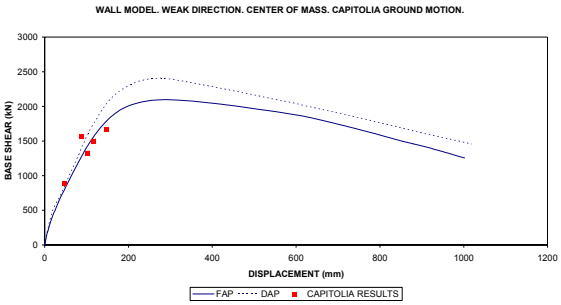

Center of mass

Figure 4.23. FAP and DAP versus Capitolia results. Weak direction. RC frame-wall model.

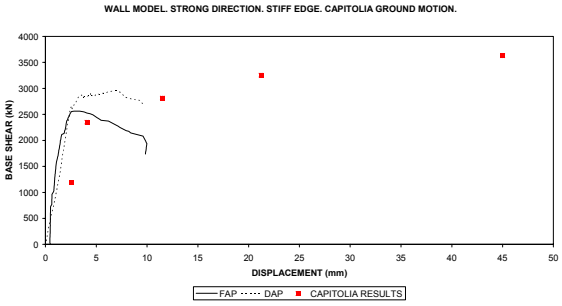

Stiff edge.

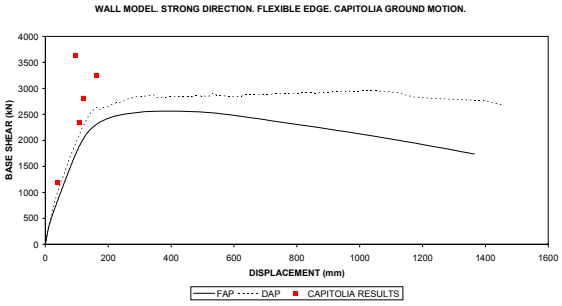

Flexible edge.

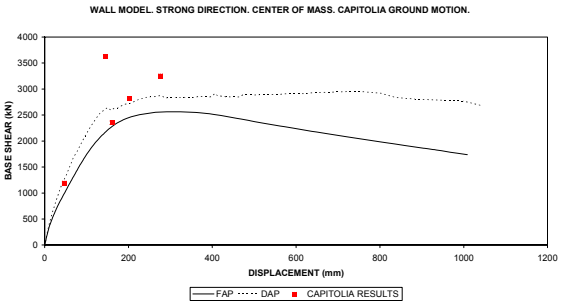

Center of mass

Figure 4.24. FAP and DAP versus Capitolia results. Strong direction. RC frame-wall model.

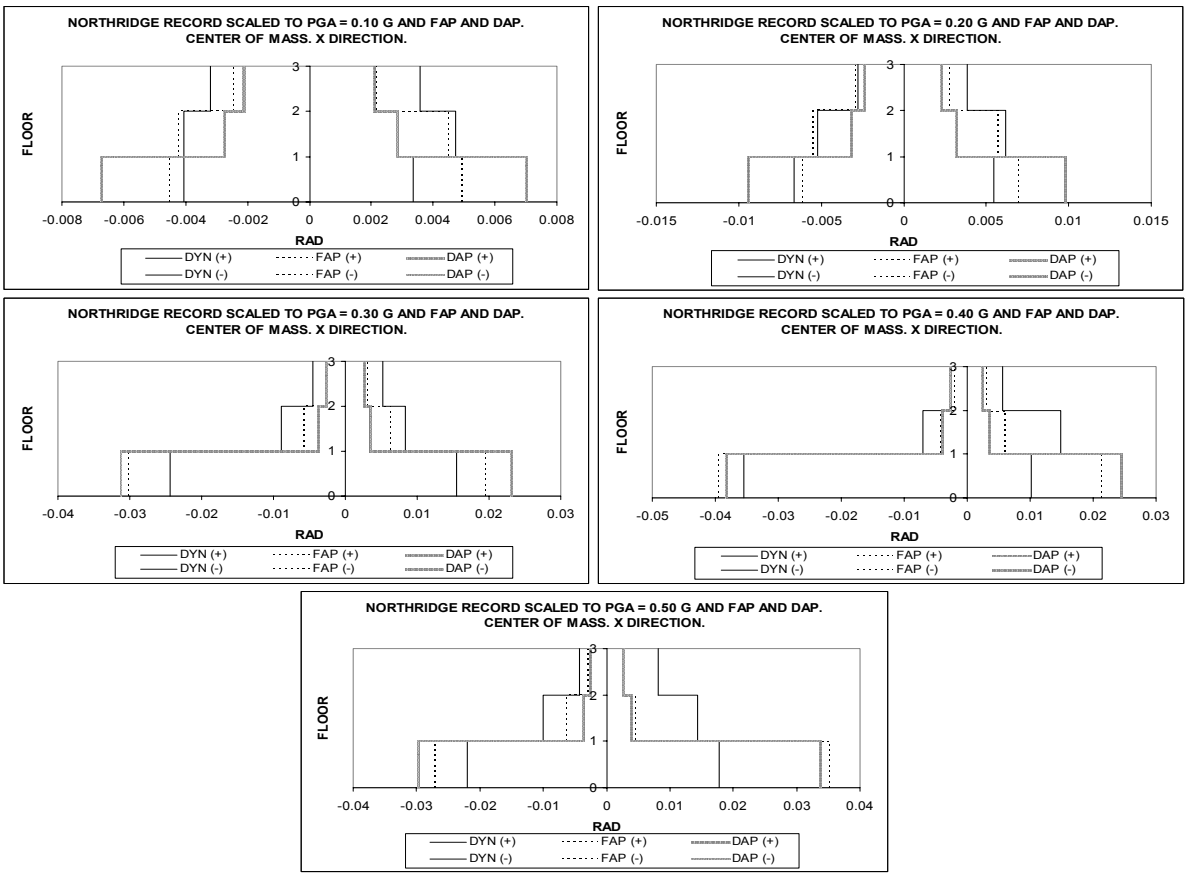

Figure 4.25. Interstory drift profiles for the Center of mass. Weak direction. SPEAR model.

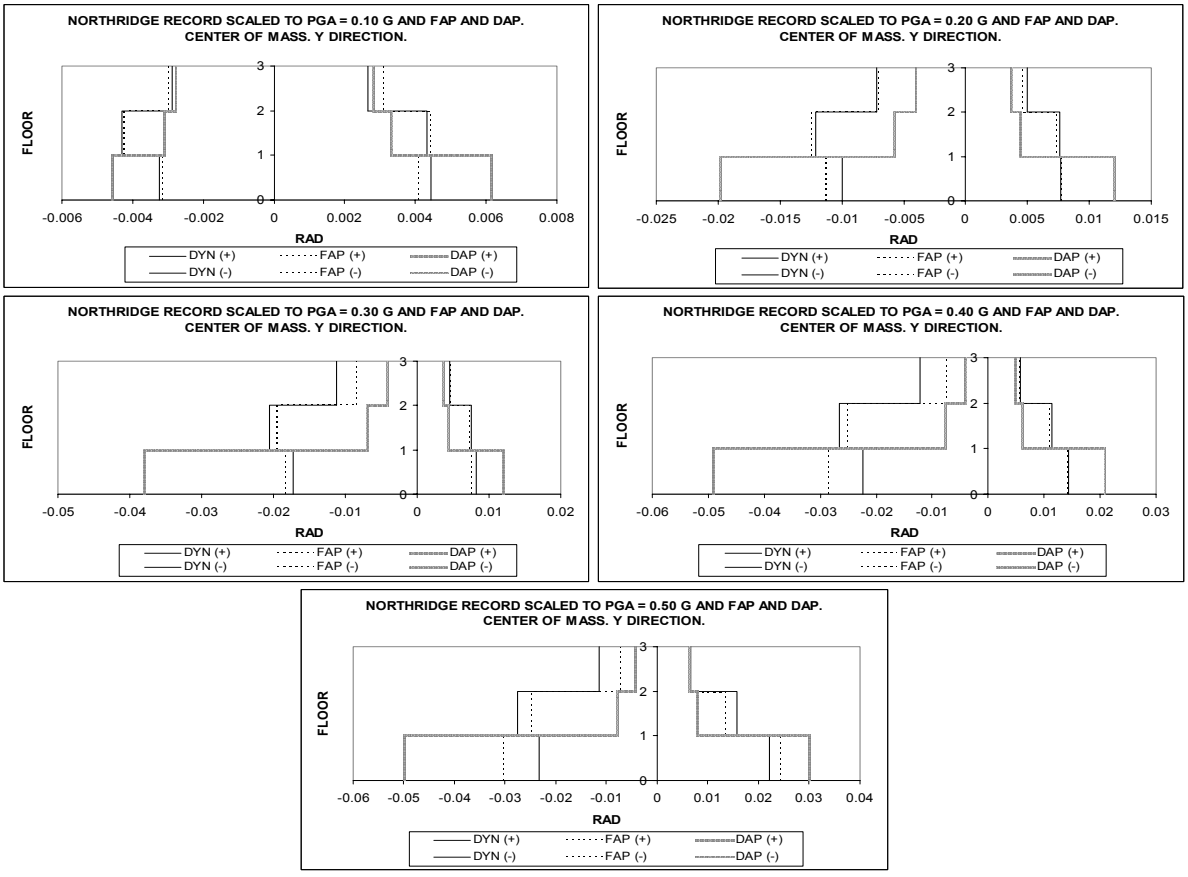

Figure 4.26. Interstory drift profiles for the Center of mass. Strong direction. SPEAR model.

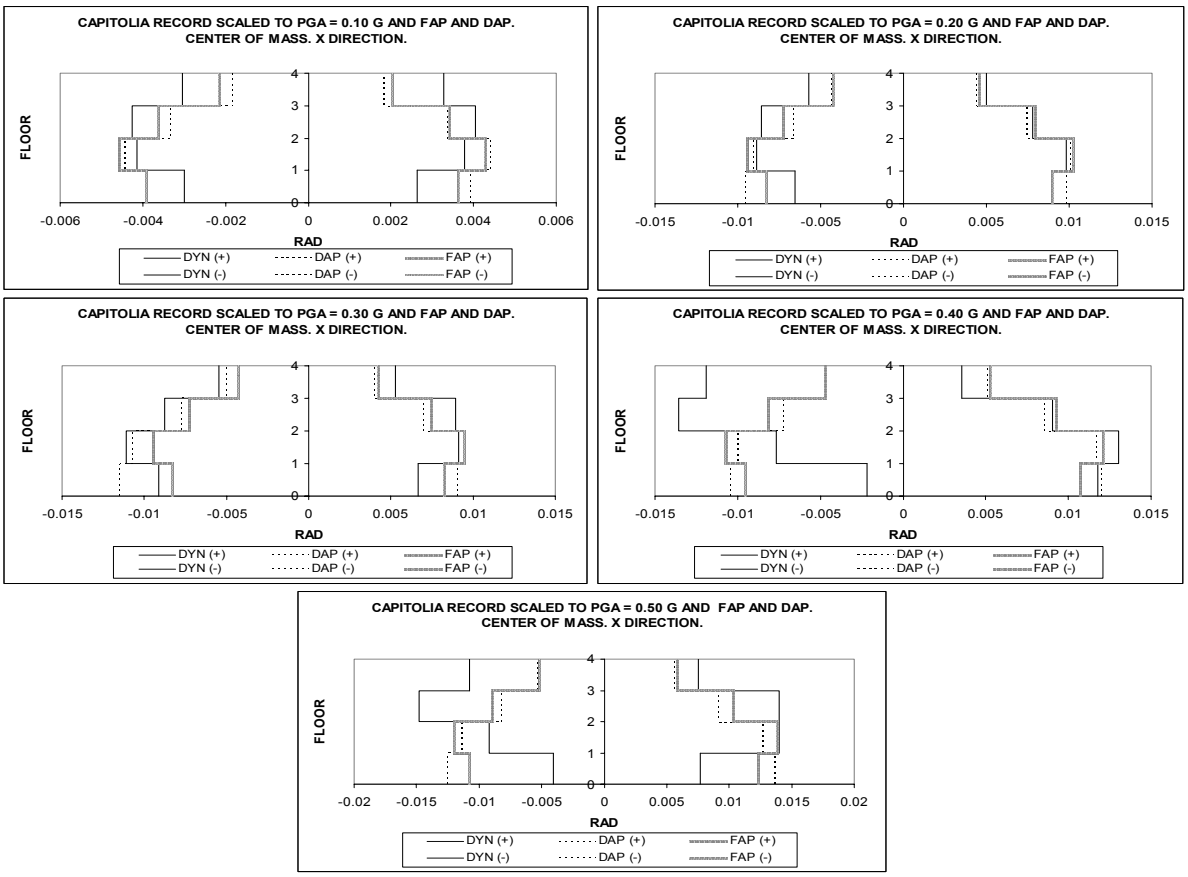

Figure 4.27. Interstory drift profiles for the Center of mass. Weak direction. RC frame-wall model.

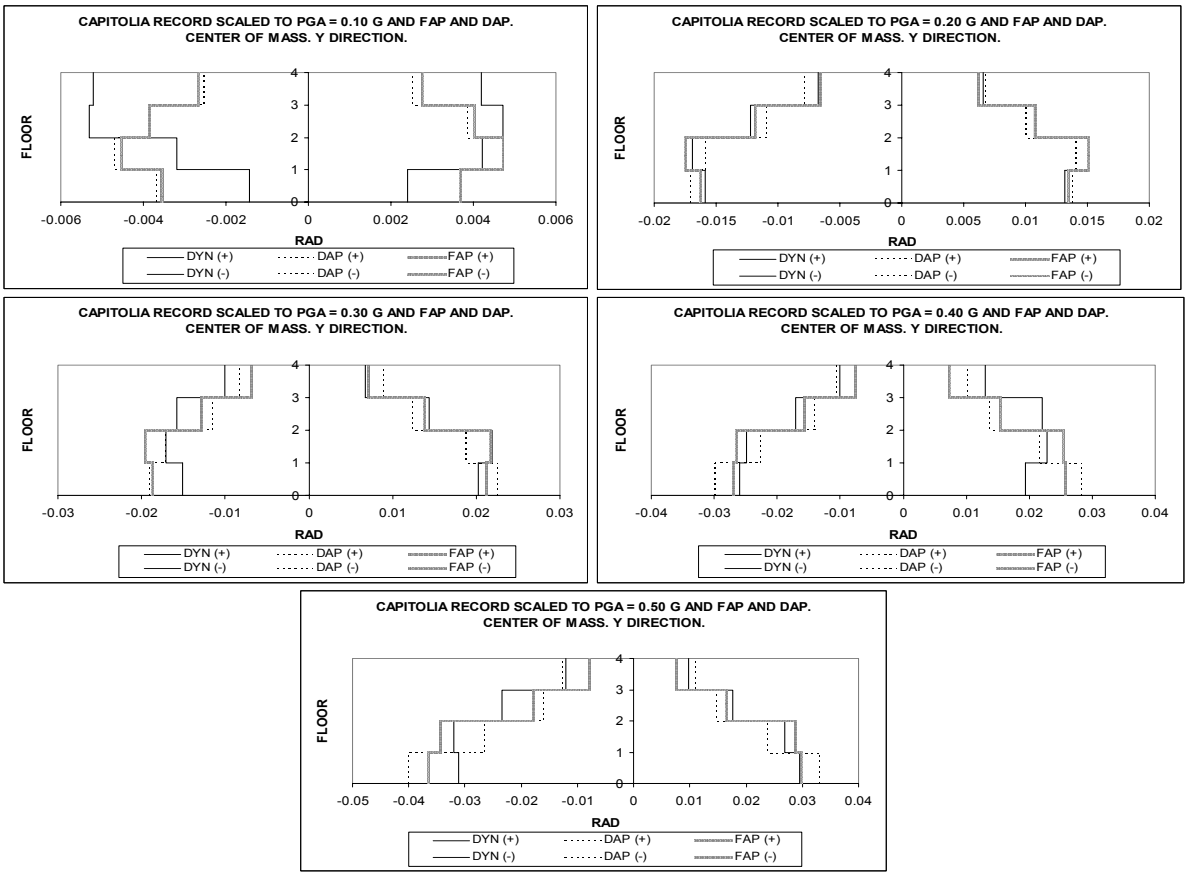

Figure 4.28. Interstory drift profiles for the Center of mass. Strong direction. RC frame-wall model.

SPEAR model. By using the capacity curves, it can be pointed out that FAP and DAP plots are very comparable between each other, when the weak direction is considered, at the center of mass and flexible edge where both pushovers agree well with the dynamic results; but, at the stiff edge DAP is a better option. On the contrary, in the strong direction, there is not a superior method between both adaptive schemes. By analyzing the interstory drift profiles, it can be stated that there is really remarkable good fitting between the FAP and dynamic interstory drift profiles in the strong direction for all the selected points and for almost all levels of intensities. In the weak direction the comparison is not as good as in the other direction, but, still, FAP is better option.

Wall model. It is difficult to select an adaptive scheme base on the pushover curves alone since the results are very comparable. From the interstory drift profiles, it can be said that at the flexible edge the interstory drift profiles show good agreement between both adaptive pushovers and the dynamic analysis in both directions. At the center of mass, profiles in the strong direction are reasonable correlated while in the weak direction the agreement is good for low levels of intensities; overall, FAP gives better matching in both cases. At the stiff edge, FAP gives slightly better correspondence, in the strong direction, than DAP; however, both adaptive schemes complete fail to predict any interstory drift in the strong direction.

It has been seen that a clear conclusion can not be drawn by comparing the pushover curves and dynamic points, only; therefore, the drift profiles have to be used to make a decision; In addition, all selected locations were also considered. Based on the all processed data, which part of it has been presented in the precedent figures, it can be pointed that FAP seems to be the correct option for the two models. Consequently, the best adaptive scheme is using the force-based methodology applying loads in a single direction. Next, the previous selection will be compared to the best conventional pushover, chosen in section 4.3.4, and to the dynamic results.

4.3.6 Comparing conventional pushover to adaptive pushover

The last step of the study is to compare the two selections made in sections 4.3.4 and 4.3.5 to the time history results; this include using capacity curves and interstory drift profiles for the two buildings. Again, two principal directions and three selected locations are analyzed; although some of the processed information is actually presented in the figures below.

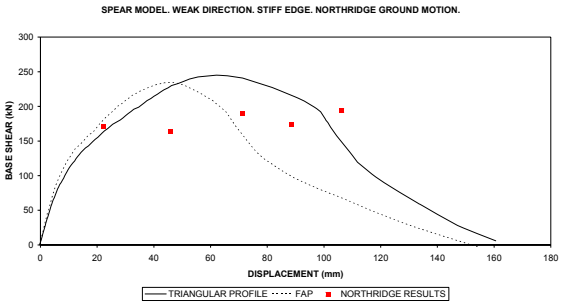

Stiff edge.

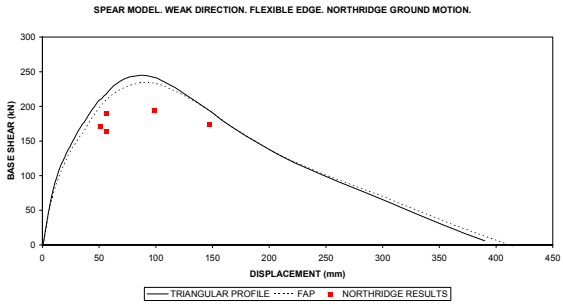

Flexible edge.

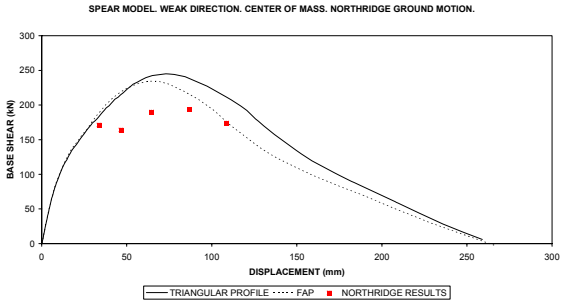

Center of mass.

Figure 4.29. Triangular conventional pushover, force adaptive pushover and dynamic results from the Northridge record. Weak direction. SPEAR model.

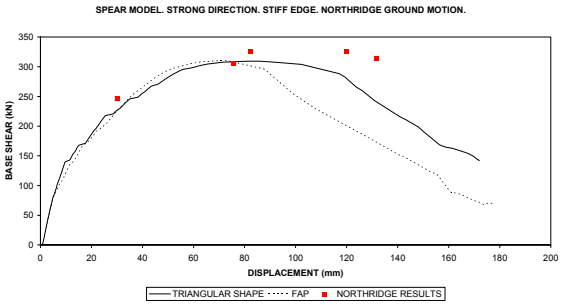

Stiff edge.

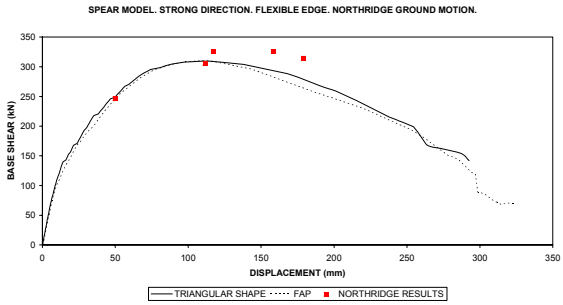

Flexible edge.

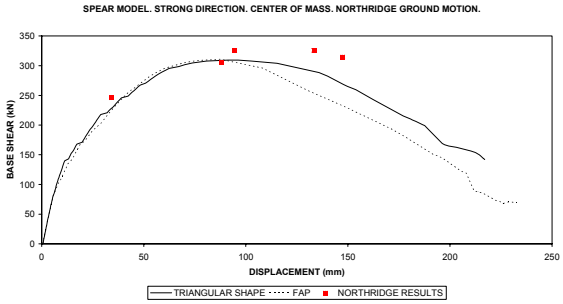

Center of mass.

Figure 4.30. Triangular conventional pushover, force adaptive pushover and dynamic results from the Northridge record. Strong direction. SPEAR model.

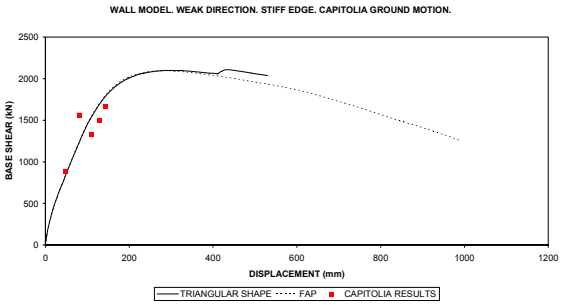

Stiff edge.

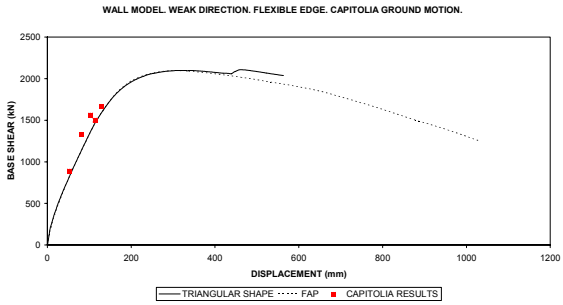

Flexible edge.

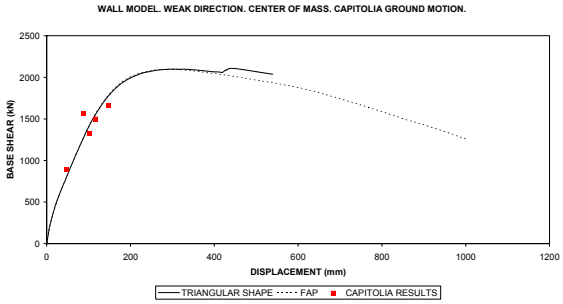

Center of mass.

Figure 4.31. Triangular conventional pushover, force adaptive pushover and dynamic results from the Capitolia record. Weak direction. RC frame-wall model.

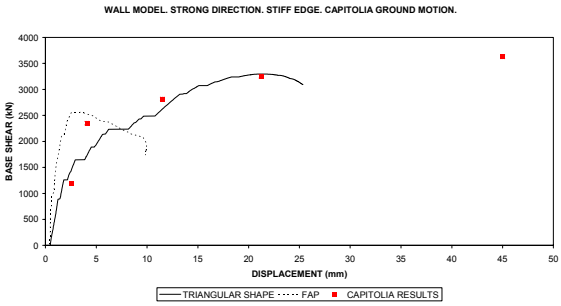

Stiff edge.

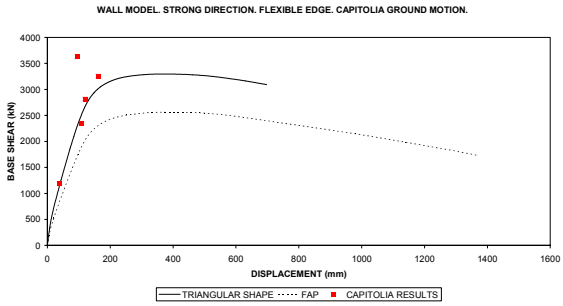

Flexible edge.

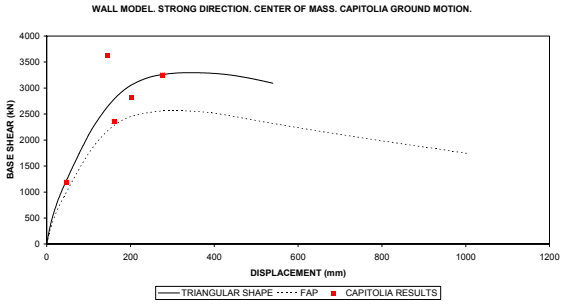

Center of mass.

Figure 4.32. Triangular conventional pushover, force adaptive pushover and dynamic results from the Capitolia record. Strong direction. RC wall-frame model.

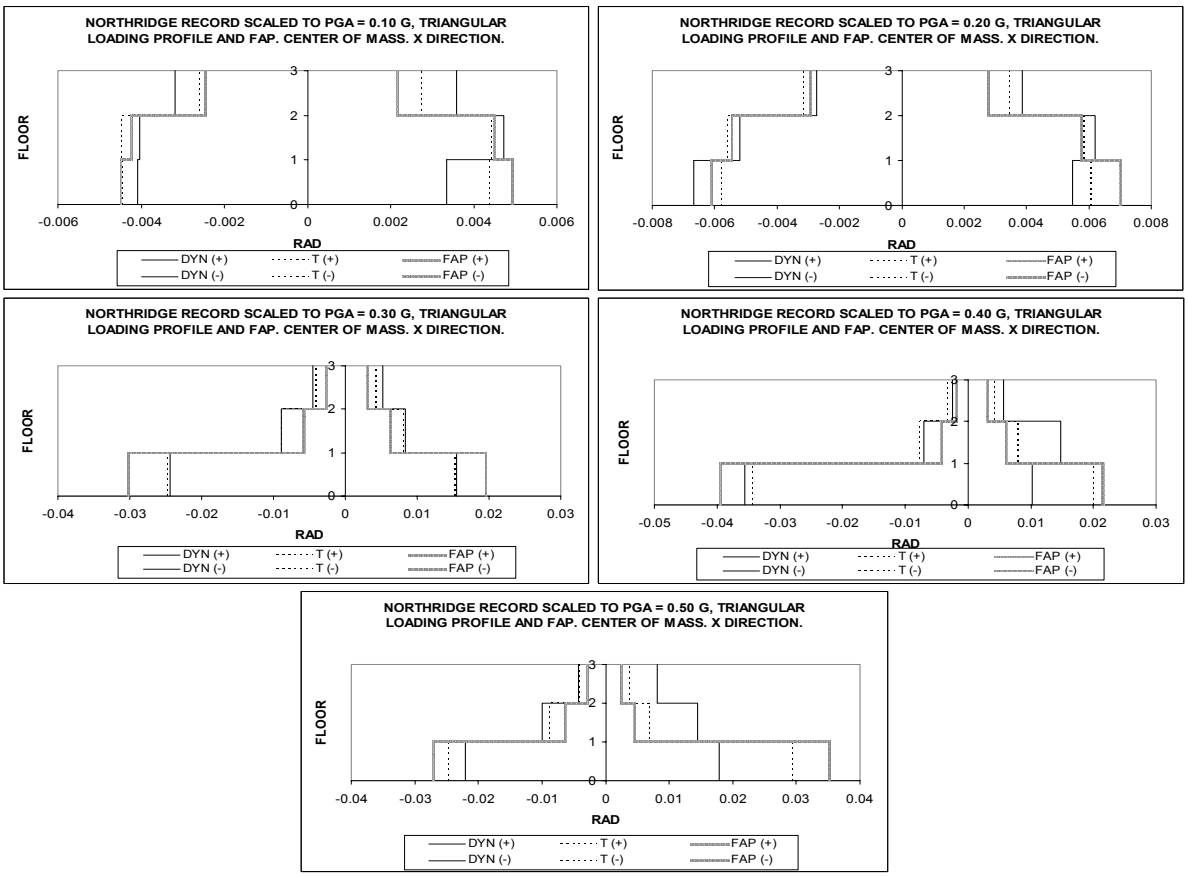

Figure 4.33. Interstory drift profiles for the Center of mass. Weak direction. SPEAR model.

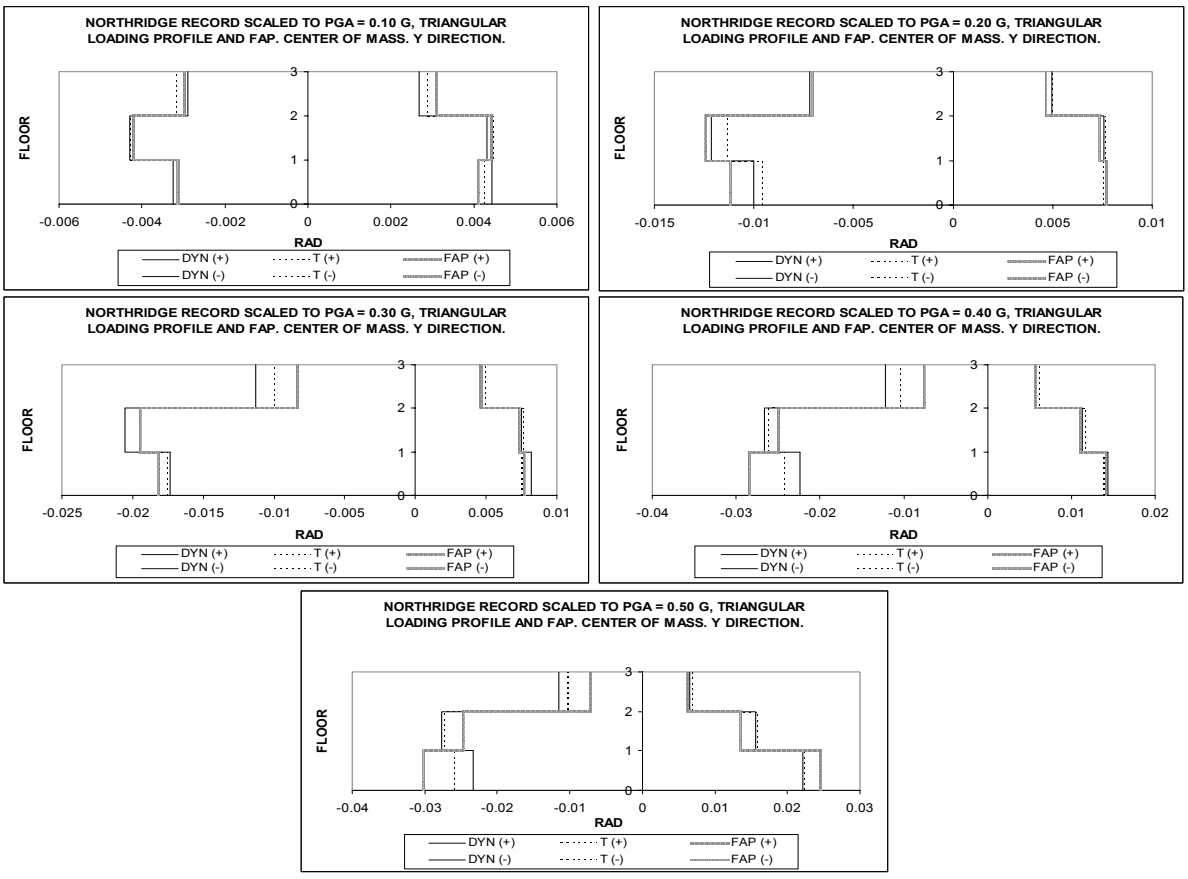

Figure 4.34. Interstory drift profiles for the Center of mass. Strong direction. SPEAR model.

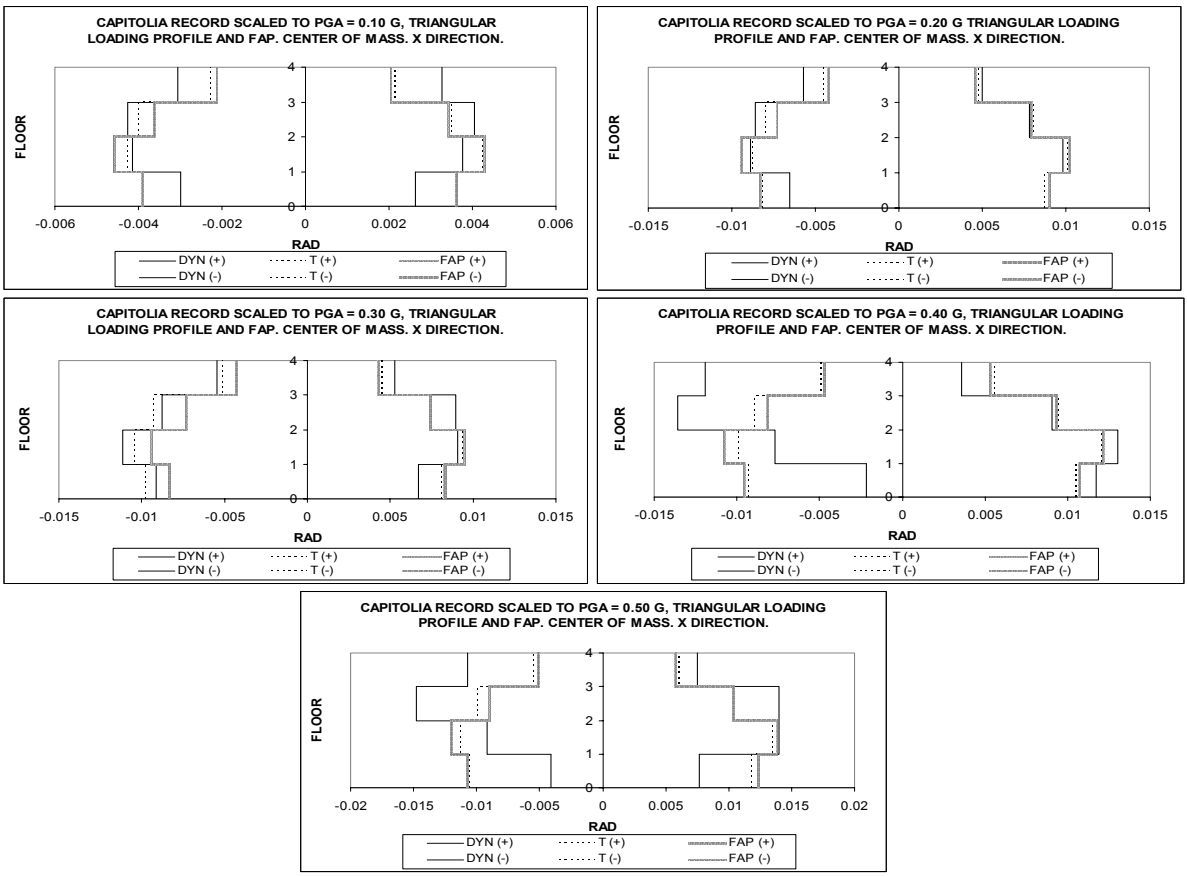

Figure 4.35. Interstory drift profiles for the Center of mass. Weak direction. RC frame-wall model.

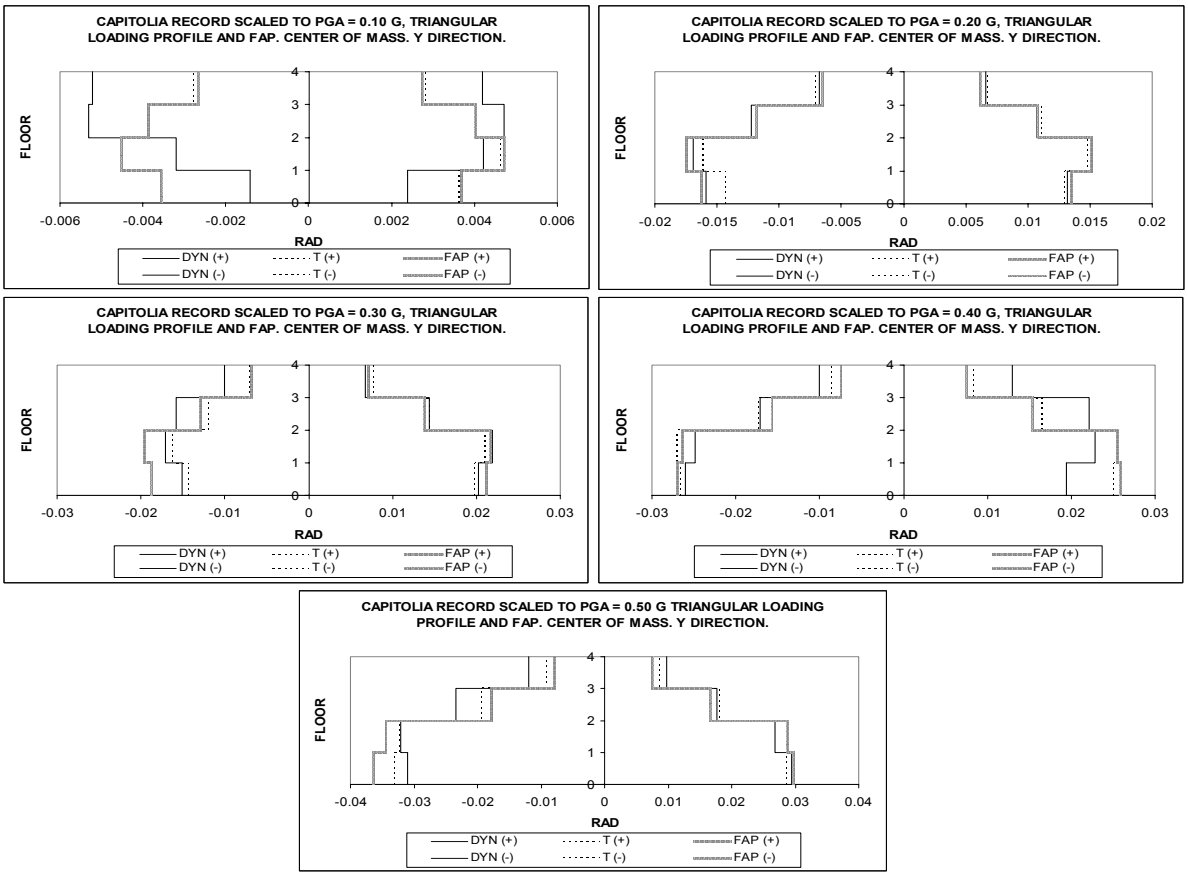

Figure 4.36. Interstory drift profiles for the Center of mass. Strong direction. RC frame-wall model.

SPEAR model. Studying the weak direction, figure 4.29, it can be said that the adaptive pushover better fits the dynamic results at the center of mass and at the flexible edge of the structure; however, it is the conventional pushover that better matches the dynamic outcome at the stiff edge. At the perpendicular direction, in contrast, conventional pushover matches the dynamic points for all levels of intensities while the FAP predicts a fast reduction in strength after passing the peak. For low levels of intensities both static approaches give good correlation with the dynamic one. It is noteworthy to point out that both static approaches provide similar strength curves at almost all analyzed points, except at the stiff edge in the weak direction where the conventional pushover predicts higher strengths than its static counterpart. If the strong direction is analyzed by using the interstory drift ratios, both, conventional and adaptive, pushovers give very good agreement with the time histories analysis with a slightly superior performance from the conventional approach. At the weak direction, both static analyses fail to accurate predict the dynamic interstory drift profiles for all intensities and studied points; but, still, the conventional pushover showed a somewhat better fitting.

RC frame-wall model. From the presented data it is not clear which approach is better. If the strength-displacement curves are considered, the weak direction there is not appreciable differences between both static approaches while in the strong direction it seems that conventional triangular pushover better suits the dynamic results. The differences between static approaches are even slimmer by examining the interstory drifts where both methodologies have almost the same merits and pitfalls in predicting the dynamic interstory drifts. Both static analyses fit the drifts remarkably well, in the strong direction, at the center of the mass and the flexible edge but they fail at the stiff edge. In the weak direction, the agreement is not as good as the perpendicular direction, but, still, the predictions are good for low and medium levels of intensities. From the precedent discussion it can be said that more study is needed to really assess the merit, or failure, from the pushover schemes.

5. CONCLUSIONS

From the information gathered in the preceding chapters the following points can be highlighted:

- The way how the slab contribution is taken into account in the mathematical discretization process produces ample variations in the predicted behavior of the model. In this research, to represent the diaphragm effect, the load applied at each level was distributed on plan considering the tributary mass acting on each node where beams and columns met. However, deeper studies must be carried out to elucidate what the appropriate way to model the in-plan behavior of floor diaphragms.
- Three different arrangements of the dynamic results (top displacement-base shear) were tried: Maximum displacement versus maximum base shear, independently of the time of occurrence; maximum displacement against corresponding base shear, using a time window of 0.5s; and maximum base shear versus corresponding displacement, using a time window of 0.5s. Those were compared to the static pushover curves, conventional and adaptive. In most cases, the dynamic arrangement that best fit the static plots is maximum base shear versus corresponding displacement, especially for the conventional pushover. The same dynamic arrangement fits the adaptive pushover acceptably well, except in those cases where the direction of analysis presents high stiffness and strength, as it is the case of walls.
- There are remarkable differences in applying loads in a single direction or in both simultaneously. In general, the strength obtained by latter procedure is always similar or less than that predicted by the former. It seems that both arrangements give comparable results in the weaker direction of the structures (composed by frames which are more or less similar), but by applying bi-directional loading predicts lesser strength in the strong axis of the systems, as it has been the case for the two building analyzed in this research. The above statement is valid by both conventional and adaptive pushovers.

- The dynamic response points lay along the pushover curves that describe the response of the structure by applying forces in one direction. This trend is confirmed by all analyses except those performed at the stiff edge where the points sometimes are closer to the bi-directional static output, sometimes lay between both static arrangement, and sometimes do not have a defined trend.
- Between the two conventional pushovers the triangular loading profile better match, in terms of both strength-displacement and interstory drifts, the dynamic outcomes. The pushover plots obtained from that profile closely match the dynamic results in both directions. On the other hand, the dynamic interstory drifts are suitably matched by that from the triangular loading shape in the strong direction of the structures, but in the weak axis the fitting is not very good for high levels of acceleration intensities.
- From the comparison between the two adaptive pushover methods it can be said that the FAP capacity curves work very well as envelope of the dynamic points, when the weak direction, of the systems, is analyzed. In the strong direction there is not a clear favorite between both adaptive schemes, but in some cases the DAP curves fit better than its adaptive counterpart the time history results. However, in the strong direction the interstory drift profiles obtained by FAP fit remarkably well those from the time history analysis. In the weak direction, FAP matches the dynamic interstory drift profiles moderately well; although, the fitting is not as good as it is in the perpendicular axis but is better than the one obtained from its adaptive counterpart.
- By comparing the conventional triangular pushover to the FAP it can be stated that, in general, the strength-displacement curves are analogous in the weak direction but dissimilar in the strong axis, where FAP predicts lower strength values. Regarding the interstory drifts, as it has been said before, both static approaches represent particularly well the dynamic drifts in the strong direction of the structural systems but they roughly characterize the dynamic ones in the weak direction. However, conventional triangular pushover provides closer results to the dynamic outcomes.
- Throughout the present research it has been shown that, for irregular buildings, by employing one location or one parameter of comparison is not enough to have an idea of the performance of the system and to choose an adequate options. The need for using at least three reference points (center of mass, stiff edge and flexible edge), to analyze the behavior of the models, has been clearly shown; in addition, the usage of both the capacity curves and interstory drift profiles has been essential to select the most appropriate alternative in most of the cases.

It is known that the number of analyzed structures is little to make any definite conclusion about the convenience of using pushover, either conventional or adaptive, to predict the behavior of irregular structures, which was the main idea behind this research. Both models are short and

similar in term of height which may not clearly highlight the high-mode effects. Thus, the following developments have to be considered as future research lines:

- More case studies have to be analyzed, especially taller irregular plan building structures.
- More accelerograms, that have different characteristics from the ones used so far, should be employed to bear the possibility of exciting different modes.
- The influence of floor diaphragm must be clearly assessed and modeled.
- Further and profound study of adaptive pushover has to be carried out.

6. REFERENCES.

1. Antoniou, S. and Pinho, R, 2003a, Advantages and limitations of the Force-based Adaptive Pushover procedure, submitted for publication.

2. Antoniou, S. and Pinho, R, 2003b, Advantages and limitations of the Displacement-based Adaptive Pushover procedure, submitted for publication.

3. De-La-Colina, J., 1999, Effects on torsion factors on simple non linear systems using fully-bidirectional analyses, Earthquake Engineering and Structural Dynamics, no. 28, p 691-706.

4. CEN, 2002, Eurocode 8: Design of structures for earthquake resistance, Part 1: General rules, seismic actions and rules for buildings, draft no. 5, Brussels: European Committee for Standardisation, Doc CEN/TC250/SC8/N317.

5. Doudoumis, I.N. and Athanatopoulou, A.M., 2001, Code provisions and analytical modelling for the in-plan flexibility of floor diaphragms in building structures, Journal of Earthquake Engineering, v. 5, no. 4, pp 565-594.

6. Faella, G. and Kilar, V., 1998, Asymmetric multistorey R/C frame structures: push-over versus nonlinear dynamic analysis, *in* Proceedings, European Conference on Earthquake Engineering, 11th, Balkema, Rotterdam.

7. Fardis, M.N., 2002, Design of an irregular building for the SPEAR project, University of Patras, 11p.

8. Filippou F.C., Popov E.P. and Bertero V.V., 1983, Modelling of R/C joints under cyclic excitations, Journal of Structural Engineering, v. 109, no. 11, pp. 2666-2684.

9. Franchin, P., Schotanus, M. and Pinto, P., 2003, Seismic assessment of the RC full-scale test structure to be tested at ELSA-JRC Ispra, Dipartimento di Ingegnieria Strutturale e Geotecnia, Università di Roma "La Sapienza".

10. Izzuddin B.A., 2001, Conceptual issues in geometrically nonlinear analysis of 3-D frames structures, Computer Methods in Applied Mechanics and Engineering, v. 191, pp. 1029-1053.

11. Kilar, V. and Fajfar, P., 1996, Simplified push-over analysis of building structures, *in* Proceedings, World Conference on Earthquake Engineering, 11th, Acapulco, paper 1011.

12. Kilar, V. and Fajfar, P., 2002, Simplified nonlinear seismic analysis of Asymmetric multistory buildings, *in* Proceedings, European Conference on Earthquake Engineering, 12th, London, paper 033.

13. Lam, N.T.K., Wilson, J.L. and Hutchinson, G.L., 1997, Review of the torsional coupling of asymmetrical wall-frame buildings, v. 19, no. 3, p. 233-246.

14. Mander J.B., Priestley M.J.N. and Park R., 1988, Theoretical stress-strain model for confined concrete, Journal of Structural Engineering, v. 114, no. 8, pp.1804-1826.

15. Martinez-Rueda, J.E. and Elnashai, A.S., 1997, Confined concrete model under cyclic load, Materials and Structures, v. 30, no. 197, pp. 139-147.

16. Menegotto M. and Pinto P.E., 1973, Method of analysis for cyclically loaded R.C. plane frames including changes in geometry and non-elastic behaviour of elements under combined normal force and bending, Symposium on the Resistance and Ultimate Deformability of Structures Anted on by Well Defined Loads, International Association for Bridge and Structural Engineering, Zurich, Switzerland, pp. 15-22.

17. Moghadam, A.S. and Tso, W.K., 1996, Damage assessment of eccentric multistory building using 3-D pushover analysis, *in* Proceedings, World Conference on Earthquake Engineering, 11th, Acapulco, paper 997.

18. Moghadam, A.S. and Tso, W.K., 2000, Pushover analysis for asymmetric and set-back multi-story buildings, *in* Proceedings, World Conference on Earthquake Engineering, 12th, Upper Hutt, paper 1093.

19. Penelis, GrG and Kappos, A.J. 2002, 3D Pushover analysis: The issue of torsion, *in* Proceedings, European Conference on Earthquake Engineering, 12th, London, paper 015.

20. SeismoStruct [2003] "Computer program for static and dynamic nonlinear analysis of frame structures" [online]. Available from URL: http://www.seismosoft.com

21. Wilkinson, S. and Thambiratnam, D., 2001, Simplified procedure for seismic analysis of asymmetric buildings, Computer and Structures, no. 79, p. 2833-2845.

DESCRIPTION OF THE 3-STOREY STRUCTURE
(THE SPEAR STRUCTURE)

Description of the 3-storey structure

The structure is a simplification of an actual 3-storey building representative of older construction in Greece, without engineered earthquake resistance. It has been designed for gravity loads alone, using the concrete design code applying in Greece between 1954 and 1995, with the construction practice and materials used in Greece in the early 70's. The structural configuration is also typical of non-earthquake-resistant construction of that period.

The storey height is 3.0m, from top to top of the slab (net storey height 2.50m under beams). The plan of the framing and the cross-sectional dimensions of members (in cms) are given in the preceding drawings. The slab thickness is 150mm.

At present time the concrete can be considered to have f_c=25MPa. The reinforcement consists of smooth bars and assumed to have as f_y the nominal yield strength (320MPa).

Design gravity loads on slabs are 0.5kN/m^2 for finishings and 2kN/m^2 for live loads.

The reinforcement of the various structural elements is given below.

Slabs: 8mm bars at 200mm centres, both ways (or equivalent welded wire mesh)

Beam Longitudinal Reinforcement

Top bars ("montage"): Two 12mm diameter bars, anchored with 180° hook at far end of column, w/o downward bent.

Bottom bars:

1. Two bars (three in Beam 4) continue straight to the supports, where they are anchored w/ 180° hook at far end of column.
2. Two (or 3 in Beam 7 or 4 in Beam 4) bars are bent up towards the supports, at locations indicated in the drawings; their bent-up ends are bent down at the far end of exterior columns and anchored w/ 180° hook at the level of the beam soffit; over interior columns they continue straight into next span, anchored at the top flange w/ 180° hook as indicated in the drawings.

Added top bars in Beams 9 and 10 over support at column C3: Two 20mm diameter bars are added at top over C3, bent-down at 45° towards the span very close to the face of C3 and anchored at beam bottom w/ 180° hooks as indicated in the drawings.

Beam stirrups

8mm diameter bars at 200mm centers, closed at top w/ 90° hooks, as indicated in the drawings. Stirrups do not continue in the joints.

Column Vertical Reinforcement and Stirrups

1. 12mm bars, as indicated in the drawings, within 8mm diameter stirrups at 250mm centers, closed w 90° hooks.
2. Clear cover of stirrups: 15mm
3. Stirrups do not continue in the joints.
4. Vertical bars are lap spliced over 400mm at floor level, including the 1st storey (w/ starter bars); spliced bars have 180° hooks.

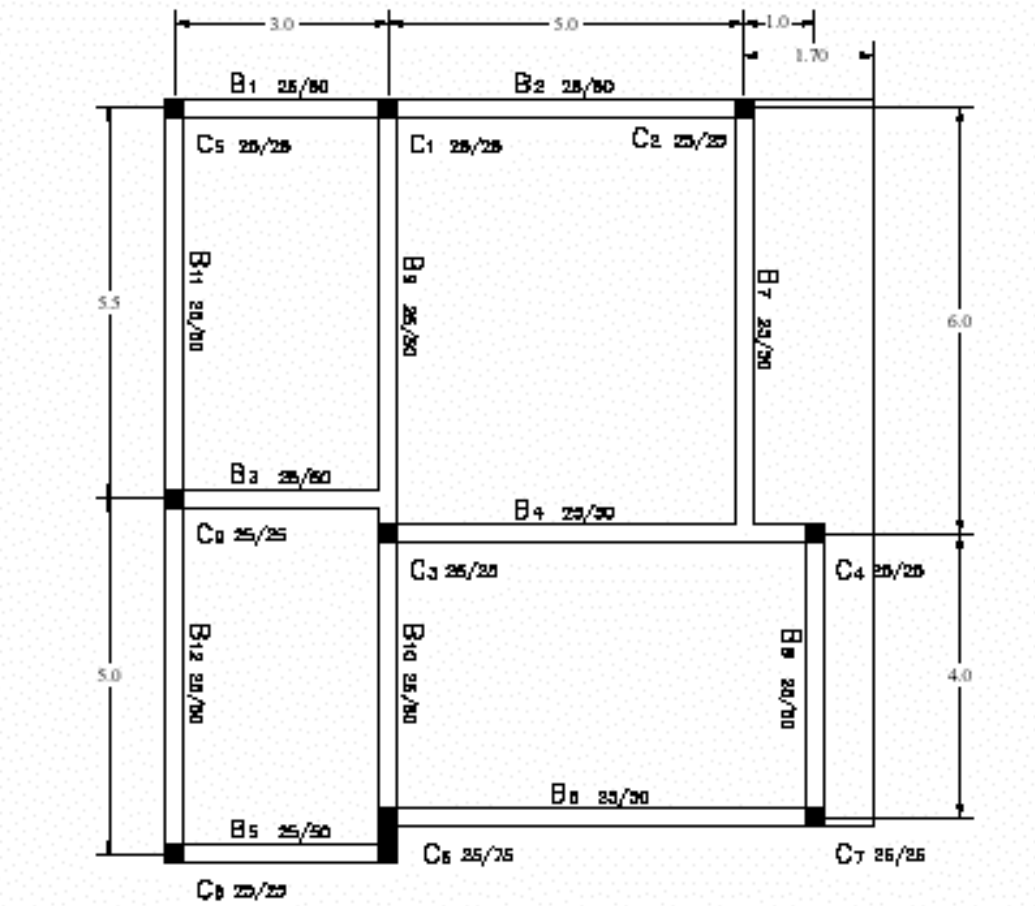
3.0
5.0
1.0
1.70
B1 25/60
B2 25/60
C5 25/25
C1 25/25
C2 25/25
B11 25/60
B9 25/60
B7 25/60
5.5
6.0
B3 25/60
B4 25/60
C8 25/25
C3 25/25
C4 25/25
B12 25/60
B10 25/60
B8 25/60
5.0
4.0
B6 25/60
B5 25/60
C6 25/75
C7 25/25
C9 25/25

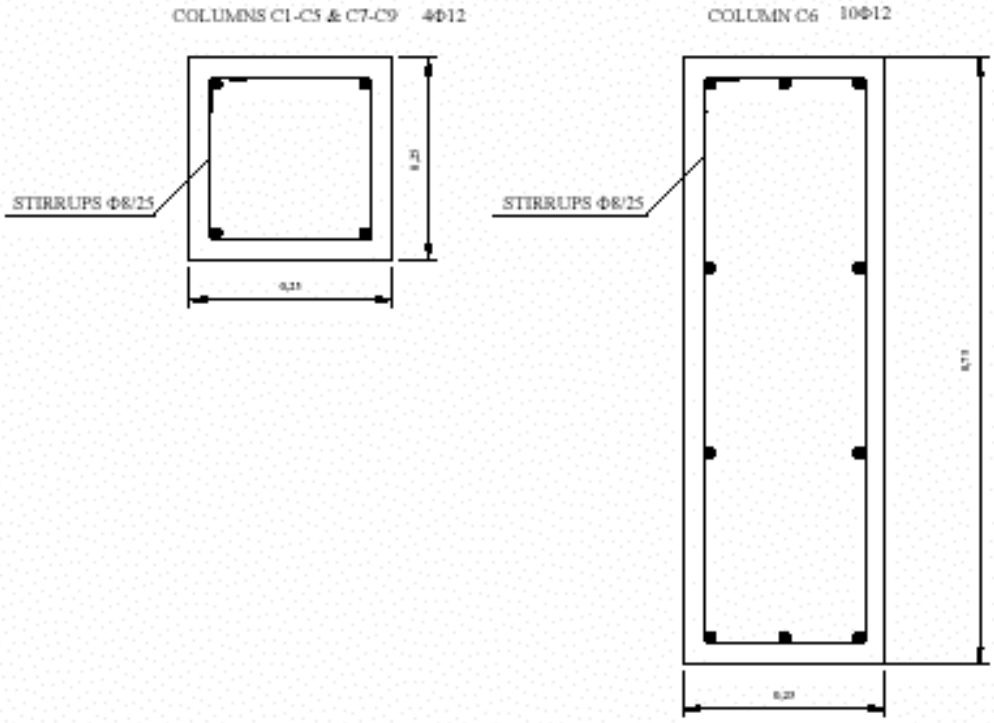
COLUMNS C1-C5 & C7-C9 4Φ12
COLUMN C6 10Φ12
STIRRUPS Φ8/25
STIRRUPS Φ8/25

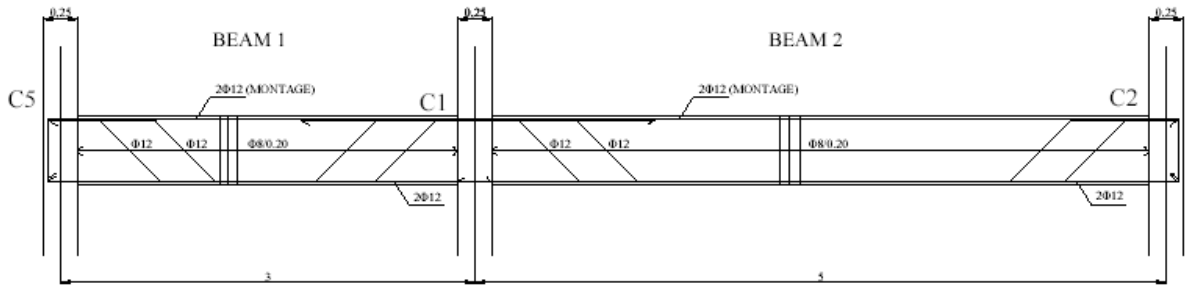
0.25
BEAM 1
0.25
BEAM 2
0.25
C5
2Φ12 (MONTAGE)
C1
2Φ12 (MONTAGE)
C2
Φ12
Φ12
Φ8/0.20
Φ12
Φ12
Φ8/0.20
2Φ12
2Φ12
3
5

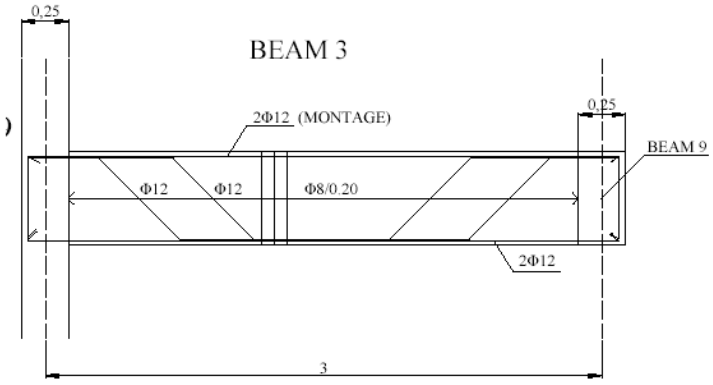
0.25
BEAM 3
2Φ12 (MONTAGE)
0.25
BEAM 9
Φ12
Φ12
Φ8/0.20
2Φ12
3

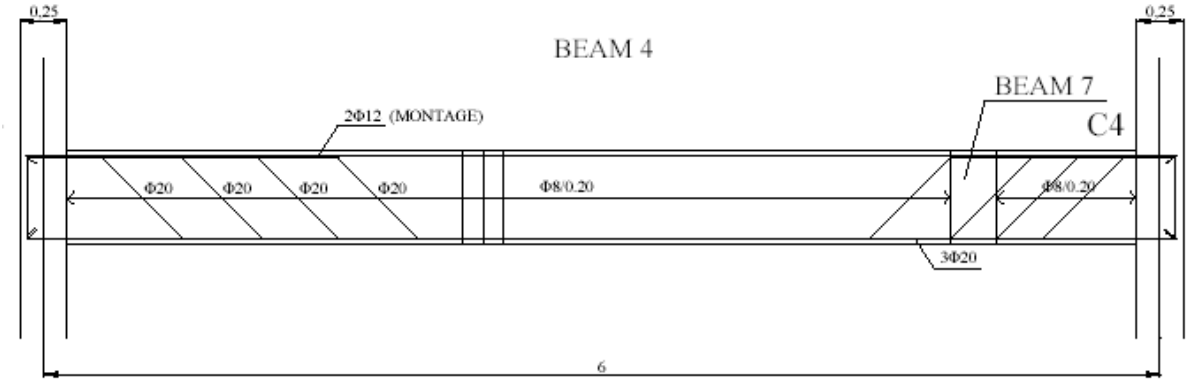
0.25
BEAM 4
0.25
BEAM 7
C4
2Φ12 (MONTAGE)
Φ20
Φ20
Φ20
Φ20
Φ8/0.20
Φ8/0.20
3Φ20
6

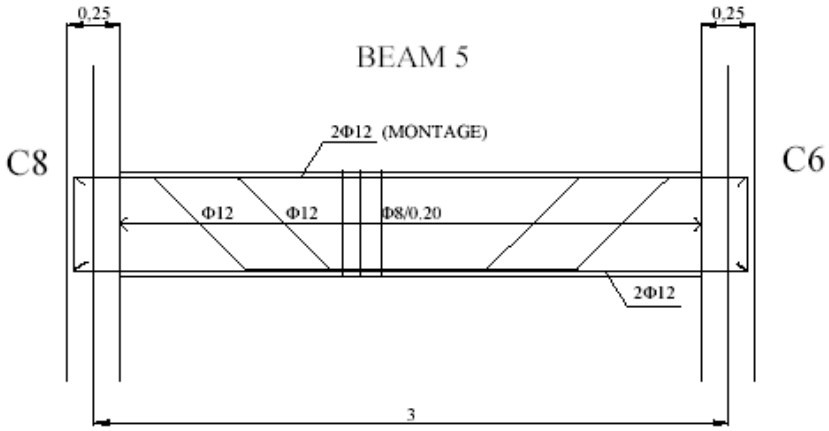
0.25
BEAM 5
0.25
C8
2Φ12 (MONTAGE)
C6
Φ12
Φ12
Φ8/0.20
2Φ12
3

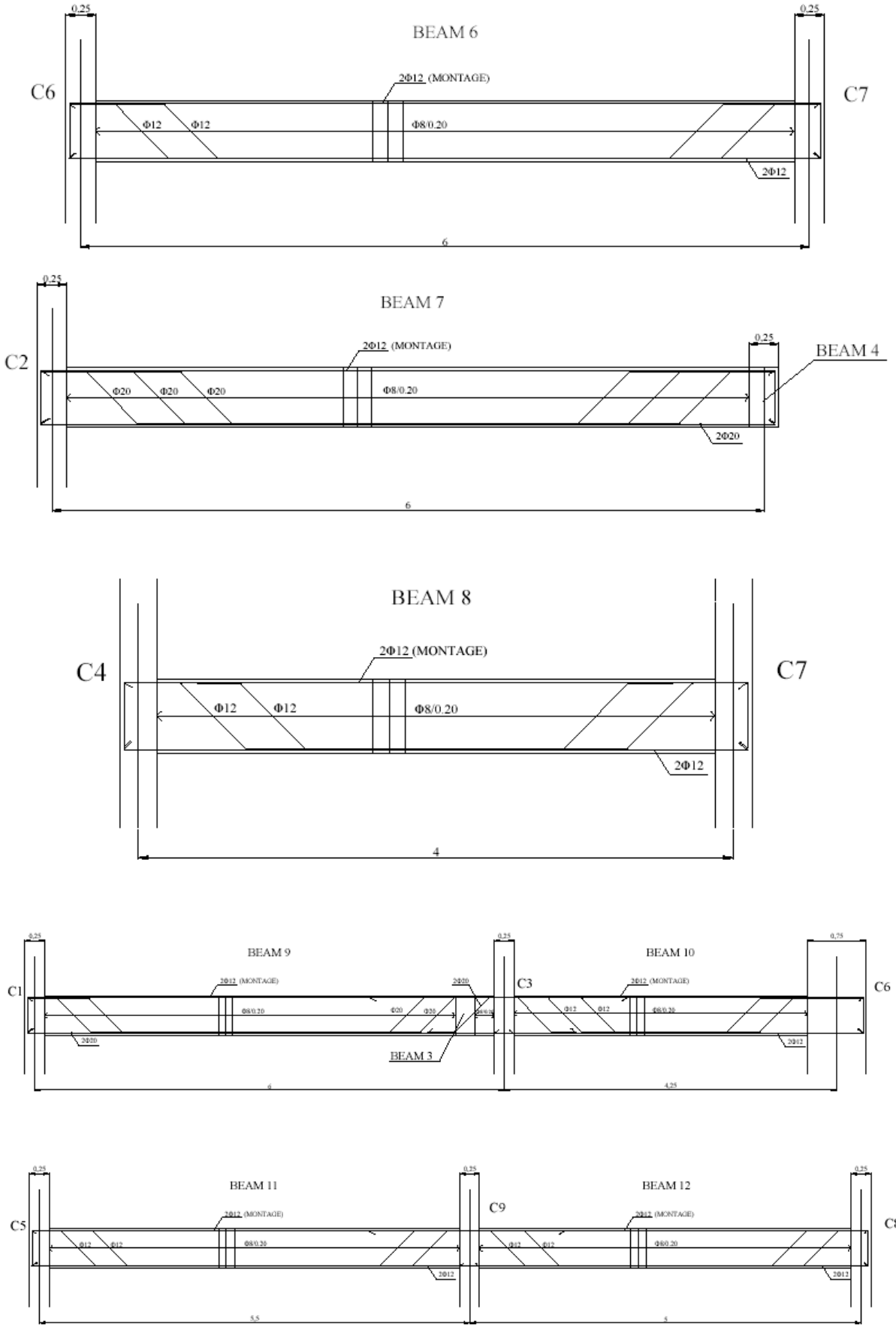
BEAM 6
C6
C7
2Φ12 (MONTAGE)
Φ12
Φ12
Φ8/0.20
2Φ12
0.25
6
BEAM 7
C2
2Φ12 (MONTAGE)
BEAM 4
Φ20
Φ20
Φ20
Φ8/0.20
2Φ20
6
BEAM 8
C4
C7
2Φ12 (MONTAGE)
Φ12
Φ12
Φ8/0.20
2Φ12
4
BEAM 9
BEAM 10
C1
C3
C6
BEAM 3
4.25
BEAM 11
BEAM 12
C5
C9
C8
5.5
5

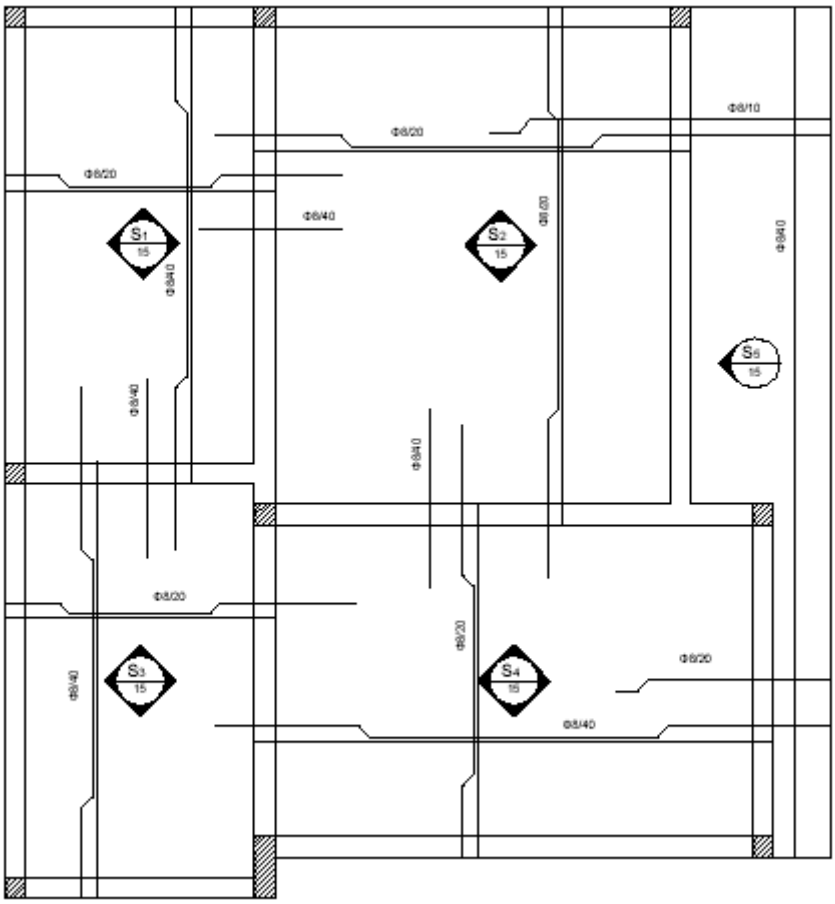
S1
15
S2
15
S3
15
S4
15
S5
15